Topology Based Optimization of Suspension and Steering Mechanisms of Automobiles

by

Reza Atashrazm

A thesis
presented to the University of Waterloo
in fulfillment of the
thesis requirement for the degree of
Master of Applied Science
in
Mechanical Engineering

Waterloo, Ontario, Canada, 2015

AUTHOR'S DECLARATION

I hereby declare that I am the sole author of this thesis. This is a true copy of the thesis, including any required final revisions, as accepted by my examiners.

I understand that my thesis may be made electronically available to the public.

Abstract

This thesis proposes a kinematic based optimization of the characteristics of suspension and steering systems by focusing on their dynamics interaction. Two of the most important suspension mechanisms are modeled. A new approach based on combining transformation matrix and vector analysis is used resulting in less time and memory consumption during optimization. Modelling is verified by comparing the results with multi-body dynamics software. Further, the steering importance and its effects on the suspension are discussed, along with modelling and analysis of the rack and pinion steering mechanism.

The optimization aims at the road holding and vehicle stability considering the effects of steering mechanism on the suspension. Therefore, the cost function is defined based on both steering and wheel travel. Moreover, the effect of wheel travel in different steering angles is shown to be important and has been considered in the cost function. In regards to some behaviors of the suspension, static constraints are defined and their importance is discussed.

Lastly, case studies are presented to provide analysis and optimization of the suspension characteristics including steering error and track alterations. Optimization is performed to design suspensions for particular vehicle classification, such as, family cars and SUVs. The results show that optimization can be used to arrive at desired behaviors when the steering and suspension interaction is considered in the optimization.

Acknowledgements

I would like to express my deepest thanks to my supervisor, Professor Amir Khajepour, who guided me patiently and his attitude was always respectful and truly.

I also would like to thank my committee members for dedicating their time to reading this thesis and attending my seminar.

I would also like to thank Dr. Avesta Goodarzi whose worthy knowledge I used and was always a great guide to me.

Dedication

To my mother, whose sleeps I disrupted. To my father, whose shoulders I bent. To my grandmother whose hands I shall kiss. And to my sister, whose passion fills me up of life.

Table of Contents

List of Figures viii
List of Tables x
Chapter 1 Introduction 1
1.1 Motivations and Challenges 2
1.2 Thesis Organization 4
Chapter 2 Literature Review 5
Chapter 3 Suspension Systems 11
3.1 Introduction 11
3.2 Suspension Function 12
3.3 Suspension Mechanisms 17
3.4 MacPherson Suspension Modelling 19
3.4.1 Equations 20
3.4.2 Steering Connection 24
3.4.3 Modelling Verification 25
3.5 Double-Wishbone Suspension Modelling 26
3.5.1 Equations 26
3.5.2 Modelling Verification 29
3.6 Anti-roll bar 31
Chapter 4 Steering System 33
4.1 Introduction 33
4.2 Technology 34
4.2.1 Modeling and Analysis 35
4.2.2 Effects on suspension design 41
4.3 Steering Kinematics 43
4.3.1 Ackermann Principle 43
4.3.2 Anti-Ackermann 45
4.3.3 Perfect steering 47
Chapter 5 Optimization 48
5.1 Introduction 48
5.2 Cost Function Definition 48

5.3 Constraints 50
5.3.1 MacPherson Suspension 50
5.3.2 Double-Wishbone Suspension 51
Chapter 6 Case Study 53
6.1 Family car 53
6.1.1 Analysis 53
6.1.2 Optimization 61
6.2 Sports car 66
6.3 SUV 74
6.3.1 Analysis 75
6.3.2 Optimization 77
Conclusion 81
Bibliography 82

List of Figures

Figure 1-Global Coordinates 12
Figure 2- "Toe in" geometry 13
Figure 3- Camber angle and Camber thrust [6,51] 14
Figure 4- Track 14
Figure 5- Kingpin inclination angle and Scrub radius 15
Figure 6- Negative Caster Angle 16
Figure 7- Solid axle suspension linked with Watt Mechanism [1] 17
Figure 8- MacPherson schematic 18
Figure 9- Double-wishbone schematic 18
Figure 10- Mercedes-Benz SLS AMG Electric Drive rear axle[52] 19
Figure 11-MacPherson Mechanism and its points' names [17] 20
Figure 12- The Model in ADAMS View and results comparison in Matlab, left, and ADAMS, right 26
Figure 13-Double-wishbone schematic geometry [53] 27
Figure 14- Double-wishbone model in MapleSim 29
Figure 15- Camber Angle in MapleSim and MATLAB 30
Figure 16- Toe Angle in MapleSim and Matlab 30
Figure 17- Anti-roll bar connection to double-wishbone suspension [54] 32
Figure 18-Anti-roll bar and MacPherson schematic [55] 32
Figure 19-Parallelogram steering [54] 34
Figure 20- Schematic of rack and pinion model 35
Figure 21-Hydraulic powered rack and pinion system [58] 37
Figure 22- Torsional bar of hydraulic valve [56] 37
Figure 23-Hydraulic assisted steering block diagram 38
Figure 24- Schematic of hydraulic assisted rack and pinion 39
Figure 25-Schematic rack and pinion connections [54] 41
Figure 26-Rack and pinion schematic with tie-rod connection inner than wheel center [56] 42
Figure 27-Rack and pinion schematic with tie-rod connection outer than wheel center [56] 43
Figure 28- Ackermann geometry [1] 43
Figure 29-Ackermann geometry [1] 44

Figure 30-Different steering geometries [1] 47
Figure 31- Toe angle changes vs. wheel travel at zero steering input 55
Figure 32-Track alterations vs. wheel travel with no steering input 56
Figure 33-Camber angle changes vs. wheel travel with no steering input 57
Figure 34- Steering characteristic of the studied car vs. Ackermann for $w = 1.7145\ m$ and $L = 2.5\ m$. 58
Figure 35- Track alterations vs. steering angle 59
Figure 36- Steering error in maximum steering vs. wheel travel 60
Figure 37-Free to change hard points 63
Figure 38- Toe angle changes (left) and Track alterations (right) by wheel travel; Comparing optimized suspension and Peugeot 405 65
Figure 39- Camber angle changes by wheel travel; Comparing optimized suspension and Peugeot 405 65
Figure 40- Points free to change for optimization 68
Figure 41- Camber by Bump at Zero Steering 70
Figure 42-Toe Changes vs Bump at zero Steering 71
Figure 43-Toe Changes vs Bump at Maximum Steering for outer wheel, left, and inner wheel, right 71
Figure 44-Track Alterations vs steering Zero Bump 72
Figure 45-Track Alterations vs Bump at zero steering 73
Figure 46-Steering characteristic of the family car and the optimized car 74
Figure 47- Initial Camber Angle variations by wheel travel 76
Figure 48-Initial guess Toe angle changes by wheel travel 76
Figure 49- Initial guess Track Alterations by Wheel travel, on the left, and Steering on the right 77
Figure 50- Toe angle Changes by Wheel Travel in maximum steering, both inner and outer wheels, and no steering 79
Figure 51- Camber angle changes by wheel travel 79
Figure 52-Track Alterations by steering 80
Figure 53- Steering Characteristics vs. Principles 80

List of Tables

Table 1- Peugeot 405 suspension dimensions 54
Table 2- Characteristics weights 61
Table 3- Weights of inputs intervals 62
Table 4- Changed vs. optimized dimensions 64
Table 5- Characteristics weights 66
Table 6- Weights of inputs intervals for Toe 67
Table 7- Weights of inputs intervals for Track and Camber 67
Table 8- Optimized dimensions and initial family car 69
Table 9- Initial SUV suspension geometry 75
Table 10-Optimized geometry vs. Initial 77

Chapter 1
Introduction

Suspension and steering have been the two main vehicular systems from the beginning of the automobile industry. The steering function lets the driver guide the vehicle. On the other hand, suspension systems serve a dual purpose. In contributing to the vehicle's road-holding, it should serve handling and braking to bring safety, and in contributing to the ride, it should keep the passengers comfortable and provide a reasonable ride quality while driving over bumps or on poor quality roads [1–3]. In other words, suspension systems should not only bring comfort to passengers within the cabin, but it should also control the movements of the wheel during travel.

Early suspensions were based on the old ox-driven cart suspensions, and they did not even use spring technology. Due to the early vehicle's low driving speeds, those suspension systems were popular and worked properly. However, after the introduction of internal combustion engines, vehicles could travel with high speeds. Old suspensions were not capable of handling forces at high speeds; therefore, newer vehicles used leaf springs in their suspension [4]. Later on, shock absorbers were introduced by Mors in France. Few years later, coil springs were introduced by The Brush Motor Company and the suspensions started to look more similar to their current state [5].

A lot of research has been done to find what characteristics play a role in performance, handling, and the stability of vehicles. Many of these characteristics, i.e. steering error, tire wear and roll, relate to suspension and steering systems and are considered to be crucial [6]. These behaviors should be optimized to satisfy the mechanical desires of a vehicle.

The introduction of coil springs was a turning point in vehicle dynamics. Requiring less space, coil springs were used in mechanisms to deliver better control over wheel movement and road holding. Two of these mechanisms, which are used widely in today's vehicle industry, are the MacPherson and the double-wishbone. These mechanisms gave the vehicle industry the opportunity to optimize the mechanical behaviors of suspension.

According to the suspension functions, studies on suspension optimization can be divided into two aspects. The first aspect is optimizing ride and comfort of a vehicle by focusing on vibration dynamics. Whereas, the second aspect targets the road holding responsibility of the suspension and tries to optimize the handling performance and safety of the vehicle. Studies on the first aim are more popular, especially that the conventional quarter car model can be used in vibration analysis and helps in simplifying the

system. As a consequence, both passive and active optimization methods can be used to satisfy the desired goal [7–9].

On the other hand, road holding optimization is more basic and is considered as the first step of suspension design. Furthermore, it affects the spring and damping ratios by providing motion ratios. Thus, it is dynamically more important to focus on this duty of suspension. These studies are even more important on steerable suspensions. The reason lies in the fact that steering affects suspension behaviors and vice versa.

Apart from the considerations noted above, steering mechanism has its own obligations that cannot be ignored in suspension design. The desired angles of steerable wheels during a turn have always been an essential case to study. This geometry requires connections that impact road holding by suspension. Accordingly, the suspension design is affected by these connections and geometries, which makes it important to consider the interaction between suspension and steering in suspension design.

All in all, amongst many different aspects of suspension design and study, optimizing its road holding abilities and minimizing undesired behaviors is crucial in suspension and steering design. In the next section, reasons that still motivate one to research this area are discussed.

1.1 Motivations and Challenges

When wheel travel happens, the wheel is forced to move and rotate in more than only one direction. This is due to the fact that the wheel is a part of the suspension mechanism. These movements introduce the characteristics of the suspension, which were previously mentioned to be important in vehicle dynamics. Therefore, studying and analyzing these characteristics are essential for designing a suspension.

On the other hand, the steering system directly moves the steerable wheels to allow the driver to guide the vehicle. As steerable wheels are related to the steering system by the suspension mechanism, the interaction between the steering and the suspension is what should be studied in optimizing those mentioned characteristics. Therefore, to provide stability and good guidance for automobiles, one should study the effect of steering on suspension characteristics as well as wheel travel.

In most of the former studies, the optimization of suspension systems has been independent of the steering effects. In those research studies, the geometry of suspension has been modified to result in a better performance by suspension during a wheel travel when no steering is applied. However, this technique of modifying the geometry may result in the steering malfunction. Another important issue is the effect of steering on the behavior of suspension in vertical movements of the wheel. During wheel

travel, the unwanted movements of the wheel are critical not only at zero steering, but also while steering is applied.

Apart from the aforementioned factors, it is essential to provide effective mechanical constraints for optimizing the suspension realistically. Static characteristics such as scrub radius and inclination angle are influential in vehicle stability and should be considered as constraints in the optimization process. In addition to all those aforementioned motivations, the type and the functionality of a vehicle is a major contributor that should be considered in suspension design. A family car may not necessarily require the performance of a racing car. However, it should be more reliable and minimize expenses.

Considering the steering effects, static characteristics and type of vehicle are essential contributions that make a study practical and motivate studies on suspension and steering.

Still, there are some serious challenges in optimizing a suspension including:

1. Developing a realistic model of suspension mechanisms to study and analyze them with high accuracy. The models should lead to a clear understanding of the behaviors of suspension.

2. Steering should be considered as another input into the suspension system along with wheel travel. Otherwise, the effect of steering cannot be considered in the optimization.

3. The cost function should include wisely chosen weights regarding the type and the functionality of the vehicle. It is important that one understand vehicle dynamics and set priorities for different characteristics; particularly, the fact that desired characteristics are not the same during wheel travel and steering either.

4. Due to the fact that optimization costs memory and computation, there ought not be too many equations that are numerically expensive to solve.

1.2 Thesis Organization

In Chapter 2 of this thesis, the relevant literature is reviewed in detail. It starts from suspension modelling and design and continues on to a literature review of the optimization of suspensions. The few studies on steering and suspension interaction are also included to indicate the strengths and weaknesses of past studies. As a result, this chapter will highlight the importance and contribution of this thesis. Chapter 3 includes suspension function and technologies with focus on MacPherson and Double-Wishbone suspension mechanisms. This chapter includes definitions of suspension characteristics with a detailed explanation of road holding duties of suspensions. Also, steering and anti-role bar connections to the suspension are considered. Then, both suspensions are modelled. The mathematical equations of the modelling introduce a new method, which is technically based on vector analysis using rotation matrixes. Results are verified via multi-body dynamics software to support the validation of the method. Chapter 4 presents an overview on the steering function and technology, and it continues on modeling an analysis of the rack and pinion. In this chapter, the kinematics of the steering and its effect on the suspension design will be studied and explained in detail. Chapter 5 defines the cost function for optimizing the characteristics along with the general physical constraints in addressing the static requirements. Chapter 6 includes case studies and demonstrates designing practical suspensions with desirable steering and road holding characteristics. All the case studies are based on engineering facts that are explained in previous chapters, and that refer to the most reliable studies. The last chapter states a conclusion about this study and points at the future research that can improve this field.

Chapter 2
Literature Review

In this chapter, former studies and experiments have been reviewed to introduce the background knowledge and research in this area. This section attempts to include most of the relevant research as well as vehicle dynamics textbooks that have affected most of these studies. Moreover, suspensions are compared, and their pros and cons are mentioned.

A comprehensive knowledge on suspension functions is of great importance to understand suspension modelling and optimization. Moreover, all the effects that it has on a vehicle's dynamics should be well studied. In this regard, many textbooks have been written. However, the focus of this thesis has been devoted on the most popular ones among researchers and engineers.

One of the most reliable references of vehicle dynamics is "The Automotive Chassis: Engineering Principles" by Reimple et al. In this reference, the types of suspension used in the vehicle industry have been reviewed. Further, the most important characteristics of a suspension system have been introduced and defined. Furthermore, the desired functions of suspension during wheel travel have been proposed in detail. The importance of toe angle, camber angle and caster angle changes are accurately explained during wheel travel [6].

In "Vehicle Dynamics: Theory and Application", Reza N. Jazar introduced suspension mechanisms by avoiding dynamical equations and focusing on the kinematic characteristics of suspension, such as caster angle and camber angle. In addition, he has provided transformation matrixes of the wheel and explained those characteristics from the mathematical point of view. In the same chapter, a detailed study on roll kinematics and geometrical requirements for a better suspension functionality has been provided [1].

Pinhas Barak has introduced some "Magic Numbers in Design of Suspensions for Passenger Cars" for optimal comfort and performance. Although his study is mostly about optimizing the dynamics of vehicles, it demonstrates how important finding and optimizing the installation factors of the spring and anti-roll bar is for allowing a simpler modelling for car suspension, which leads to a better suspension performance [10]. In this regard, the motion ratios that play a role in making mechanical modelling easier are defined and studied in this thesis.

The two-dimensional simulation of the suspension mechanism is a simple way to study its non-linear behavior. Therefore, the focus of many studies has been devoted on this approach, and the results show the acceptable accuracy of this method. Camber angle, roll center and inclination angle are three important characteristics that can be studied in this type of modelling as well.

Stensson et al. have studied the importance of nonlinear modelling of a MacPherson suspension in "The Nonlinear Behaviour of a MacPherson Strut Wheel Suspension" [11]. They have modelled a two-dimensional MacPherson suspension by three different methods. Then, they have stated the importance of the nonlinear modelling by a comparison between these models and the real test rig results. This article shows the crucial role of a precise kinematic analysis in improving the dynamic study of suspension [11].
J. Hurel et al. have performed another two-dimensional study of a suspension mechanism in 2012. The paper proposes a nonlinear modelling of the MacPherson strut, and it uses the Matlab-Simulink to simulate the model. It also has compared the results with ADAMS [12]. In this study, they used the transformation matrix method to model the MacPherson mechanism, which had been previously used, in 2009, by M.S. Fallah et al. The paper proposed the very same approach in modelling the MacPherson suspension by providing detailed mathematical equations. They have not only validated the results using ADAMS software, but also provided the comparison of the nonlinear model with linearized and conventional quarter car model. M.S. Fallah et al. have also used linearized equations to control the system [13].
E. R. Anderson has done a full modelling of the MacPherson suspension in a Master's thesis. The study includes the two-dimensional modelling of the system, and has compered the results with both conventional quarter car model and test rig experiment results. Subsequently, system identification has been proposed based on the developed model for control approaches [14].
Although all the two-dimensional modelling of suspension systems, which are applied in many studies, are in acceptable accordance with ADAMS multi-body models, they cannot yield one of the most important road holding characteristics of the suspension: toe angle changes, which refer to the rotation of the wheel along the vertical axis. Toe changes by wheel travel can cause unwanted steering forces while driving over bumps. This phenomenon, which is also known as bump-steer, is one of the most non-desirable movements of the wheel. Furthermore, wheel travel also happens by turning and toe changes can cause roll steer. Generally, these alterations can cause steering error and should be studied accurately. According to many studies, the most desirable situation is the entire lack of toe angle variation [6,15,16].
As mentioned, three-dimensional modelling of suspension systems play a great role in both analysis and optimal design of the suspension. One of the comprehensive studies on three-dimensional suspensions is proposed by M. S. Fallah et al. The paper has used a three-dimensional transformation matrix method to study the suspension's behavior. Then, by applying physical constraints of joints, 18 equations are provided for solving the AE equations. For an easier velocity and acceleration solve, the equations of motion from degrees one and two are linearized. Track alterations, toe and camber angle alterations are all

considered as the most important behaviors of suspension kinematics. This paper also proposes an energy method to analyze the dynamics of the MacPherson strut. Moreover, a case study is done on a vehicle, and the results are compared with other automobiles for a complete analysis [17].

H.G. Lee et al. also have studied the 3D kinematics of the MacPherson mechanism. In this study, except for an R-S link constraint, no other equations are provided for kinematic modelling. The analysis is focused on the constraints of optimization and also changes in characteristics during jounce and rebound. In the paper, a sensitivity study was done on characteristics regarding the hard points of the mechanism. Also, the importance of track alteration is neglected and kingpin angle variation is considered to be as important as toe changes [18]. However, in most vehicle dynamics textbooks, toe angle plays a significant role in the stability of vehicles, and the kingpin angle plays role in steering issues. These were not considered in the study at all [2,6,16]. Further, the kingpin angle is not independent from the caster angle and the inclination angle, which could be considered as a static constraint for a better dynamics in vehicle[6].

Amongst studies on suspensions' 3D modellings, H. A. Attia proposes a modelling for front suspension double-wishbone linkage by using the "point and joint coordinate" method to formulate the system. This method yields 11 equations to be solved, and in this regard, it is one of the most efficient dynamic studies on a suspension system [19].

In a study by X. Liu et al., the effects of the coordinates of double-wishbone hard points are studied based on correlation theory. The main purpose of this study is to analyze the effect of hard points on the optimization of a SAE formula one, which is mostly focused on performance, rather than ride characteristics. Therefore, the kinematic behavior of the suspension is the main interest of the paper [20]. The authors have not provided detailed equations for their modelling process.

By reviewing the formerly discussed literatures carefully, it can be realized that all studies have focused on suspensions with kinematical degrees of freedom, and the effect of bushings are ignored [17,21]. However, studies have been done on multi-link suspensions that are dependent on bushings as well. Although the analyses of these suspensions are not a subject of interest in this thesis, the optimizations are important from the engineering point of view. J. Knapczyk and M. Maniowski propose a detailed modelling for studying a five-rod multilink suspension with sub-frame [22]. Later, they use the same study to optimize a five-rod multilink. However, the optimization is focused on dynamical characteristics of the suspension [23].

In addition, P. A. Simionescu and D. Beale propose a synthesis for the five-link rear suspension. Their study is focused not only on analyzing the multilink suspension, but also on the optimization of kinematic

characteristics of the suspension [16]. Moreover, the optimization in this paper is based on reasonable engineering factors, rather than optimization rationales for many other studies. These factors are in accordance with studies on linkage suspensions, which clarify the unity of desired behaviors in all kinds of suspension mechanisms.

On the other hand, some studies have tried to develop a general method for suspension synthesis instead of focusing on a certain mechanism. S. Bae et al. use an axiomatic study to design MacPherson, double-wishbone and multilink suspensions. The study presents the kinematic design of the mentioned suspensions by analyzing the effects of suspension hard points on some "functional requirements" [24].

In regards to the optimal design of suspension mechanisms, multi-objective optimizing of a double-wishbone mechanism was an interest of J. S. Hwang et al. By using genetic algorithm and considering two categories of suspension: stability and controllability, a multi-objective optimization was performed to find the optimal geometry of the suspension. The paper proposes a displacement matrix method for modelling the double-wishbone suspension [25].

R. Sancibrian et al. have also used a multi-objective approach in optimizing a double-wishbone suspension. However, they have provided a detailed formulation of the mechanism. The modelling approach is based on considering all the links as a rigid body and providing enough constraints to solve 24 equations for the system. This modelling method is one of the most widely used methods that can be found in many multi-body dynamics textbooks [26–28]. Moreover, a detailed description of the cost function is provided and the optimization is based on "gradient determination using exact differentiation" [29]. However, the desired characteristics are not in a full accordance with many vehicle dynamics studies [6,15,16].

Steering kinematics is an important matter of study and design in vehicle dynamics. Although steering is affected by suspension's geometry, a comprehensive knowledge on the steering function and technology is required. Accessing this knowledge requires the reviewing of textbooks and research papers on steering principles and their pros and cons.

In "Vehicle Dynamics: Theory and Application" by Reza N. Jazar, a detailed study has been done on the steering kinematics. The Ackermann steering principle is analyzed along with curves that show the effect of steering geometry having a more accurate Ackermann kinematics while steering. In the same chapter, it also indicates the anti-Ackermann and parallel steering geometries, and a brief comparison between those and Ackermann is provided [1].

In one of the most impressive studies of steering kinematics, Dale Thompson has introduced the fundamentals of steering kinematics. There, the pros and cons of anti-Ackermann steering have been

summarized with a complete literature review. Furthermore, results have been shown to prove the paper's statement about anti-Ackermann effects on vehicle's handling [30].

According to Dale Thompson, Costin and Phipps [31], Carrol Smith [32,33], and Allan Staniforth [34] have recommended anti-Ackermann steering for racing and sport cars. On the other hand, Don Alexander [35] and Paul Valkenburg [36] have not directly recommended anti-Ackermann kinematics. However, they believe it has positive effects on competition cars. On the contrary, Eric Zapletal writes the only racing car textbook that has not focused on anti-Ackermann steering or its effects on steering. The reason is issued to Vehicle Stability Programs being used in modern cars [37].

Claude Rouelle also provides analysis to support the anti-Ackermann steering for higher performance. He believes that using static toe out and reverse-Ackermann steering is the best setting for racing cars [38]. Mark Ortiz also believes that anti-Ackermann along with initial toe out is effective for racing vehicles [39].

In a study on steering that focuses on the Ackermann principle, an optimization of steering geometry has been proposed by I. Preda et al. to satisfy a pro-Ackermann steering. The MacPherson and the rack and pinion cooperating system has been studied by planar modelling, and the 2-D optimized results have been modelled in Catia-V5 in 3D to analyze the results [40].

The interaction between steering and suspension is very important when optimal design is of interest. Therefore, the effects of these two systems on each other should be reviewed. In "The Automotive Chassis" by Reimple et al., the Ackermann principle has been introduced and steering effects on the variations of camber, kingpin and inclination angles are explained and justified in detail. It has also elucidated the effects of static characteristics, such as scrub radius and roll center on vehicle's dynamics [6].

Moreover, different steering mechanisms and their pros and cons are discussed. Power assisted steering systems are introduced and explained in details with engineering schematics of parts and connections. Then, it is shown that mechanical requirements introduce some geometrical constraints in suspension and tie-rod designing to satisfy desired characteristics [6].

Considering the interaction between steering and suspension, P. Simionescu and D. Beale in "Synthesis and analysis of the five-link rear suspension system used in automobiles" explain the requirements of a well-designed suspension. They defined their synthesis problem by introducing kinematic conditions that satisfy those requirements. Also, by referring to Raghavan's "Suspension kinematic structure for passive control of vehicle attitude", they explained how important it is for a suspension system to avoid any

movements other than vertical displacement of the wheel during wheel travel [15]. In the same study, a more optimal design is provided for a known suspension [16].

S. Park and J. Sohn have studied the importance of camber angle in steering, and they have tried to control its front suspension changes. In this study, the effects of camber angle in steering have been discussed, and it has been shown to have a slight effect on producing lateral forces [41]. Therefore, camber alterations during wheel travel should be small so that the stability of vehicle is not negatively affected. This study also indicates another steering characteristic that plays a role in suspension design.

Although there are few studies on the front suspension that has included the steering effect on suspension characteristics, D. A. Mantaras et al. have proposed a three-dimensional kinematic model for a MacPherson mechanism that considered the steering as well. The modelling method is based on the transformation matrix of the wheel and constraint analysis of each link. After the process of modelling, the equations have been solved in MATLAB and the model is validated with a real test rig experiment [21].

As one of the most important behaviors of suspension is providing the stability while wheel travel, steering error must be minimized. M. L. Felzien and D. L. Cronin have studied and optimized the steering error of the MacPherson strut. This study has included the steering input to the MacPherson mechanism, which is provided by a rack and pinion steering mechanism. The steering kinematics is considered to be a parallel steering and the optimization is focused on minimizing the steering error while wheel travel happens in cornering. The paper shows the importance of considering steering in kinematic analysis of the suspension very well [42].

Another research on improving a MacPherson suspension system which has considered the topic of steering is by H. Habibi et al. Authors have tried to minimize the undesired “roll-steer” by considering the body roll of a vehicle in turning and using the genetic algorithm. Not only is the change of toe by roll considered to be important, but camber and caster variations are also kept minimized. This shows the study’s respect to vehicle dynamics. The 3D modelling of the MacPherson system is based on closed geometrical loops and yields only 13 equations to be solved [43].

In conclusion, amongst all studies and research on suspension and steering, there still is a lack of comprehensive study that considers both of these systems in optimizing road holding responsibility of the suspension. In this thesis, individual characteristics of steering and suspension along with dependent behaviors, such as steering error, have been analyzed and optimized from the engineering point of view. Furthermore, a new approach has been used in modelling the suspension mechanism to reduce the number of equations.

Chapter 3
Suspension Systems

3.1 Introduction

A suspension is a system of links, springs, and dampers that allow a relative motion between body and wheel [1]. Suspension systems should provide vehicle safety during wheel travel and steering, and these systems should also aid in creating a comfortable ride for passengers. When it comes to steering, the suspension systems of the front and the rear of a car are usually different.

In front suspensions, the lack of stability, tire erosion and bump-steer are unwanted results of a poor designed suspension. Therefore, there have been many studies on those characteristics that play main roles in increasing stability and reliability of a suspension. There are mechanisms that help preventing undesired movements of wheels, and lead vehicles toward having an optimum road holding performance. For instance, according to many vehicle dynamic studies, bump steer causes stability issues and should be totally prevented [1,2,6].

Two of the best and most widely used mechanisms of suspension are the double-wishbone and MacPherson mechanisms. In the automotive industry, the double-wishbone suspension was introduced by the Citroen Company in 1934 in Rosalie and Traction Avant models [44]. Although it is more complex and takes up more space than a MacPherson, it can be optimized and is easier to fine-tune. The MacPherson mechanism was supposed to be introduced in Chevrolet Cadet as a light-weight vehicle by Earle S. MacPherson in 1945. However, the Cadet project was cancelled and the strut patented in 1947 [45]. This suspension requires smaller space and fewer links, and it is also fair in being tuned and optimized for its wheel travel characteristics. Thus, the MacPherson strut is very popular in vehicle industry.

In this chapter, the analysis of both abovementioned suspensions in relation to the standard characteristics of suspensions is provided. This analysis is used in the optimization chapter for finding the optimal positions of the mounting points to the chassis and the positions of linkage connections. Steering effects and the relation between steering mechanism and the suspension is also considered in the modelling.

3.2 Suspension Function

The suspension has two important responsibilities in a vehicle: ride comfort and road holding. Ride comfort is important in regards to preventing harsh impacts to the human body and any luggage while driving. For instance, the human body's sensitivity to vibrations from 2 to 10 Hz is greater [46–48], and certain frequencies can cause whirling sensations or overlap with body part resonances [10]. Thus, the suspension should prevent vibrations in zones such as a vehicle's seat. On the other hand, road holding shows a crucial effect on vehicle safety, handling, and performance. The focus of this thesis is also devoted to this service of suspensions. Therefore, the characteristics that play a role in this regard should be reviewed.

The first step is to define vehicle coordinates. According ISO 4130 and DIN 70000, the standard coordinates of a vehicle are shown in Figure 1[6].

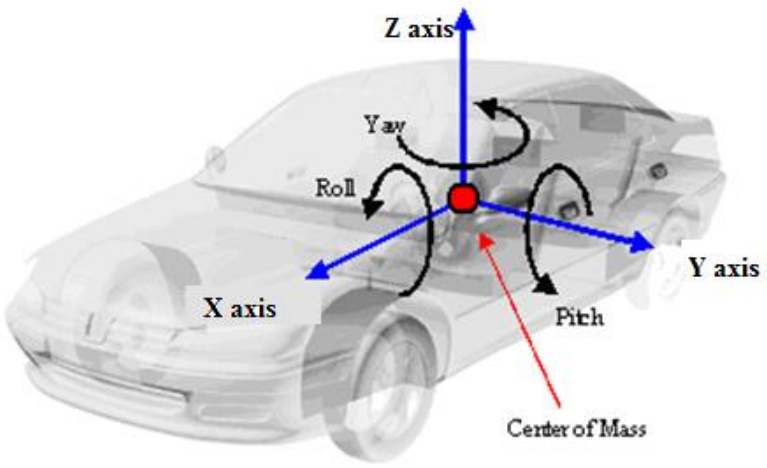

Figure 1-Global Coordinates

The toe angle is the angle between the steerable wheels' longitudinal centerline and the vehicles' longitudinal centerline viewed from top. Figure 2 shows the definition of the toe angle. The variations of this angle by bump, roll or any other input could impact vehicle performance. This is due to the fact that the major amount of the lateral force for steering is produced by the slip angle of tire [2,6]. A simple

popular estimation of the slip angle of the steerable wheels in normal steering conditions and small slip angles is as below.

$$\alpha_f = \delta - \frac{v + ar}{u} \qquad \textbf{(3-1)}$$

In the above equation, δ is the amount of steering angle on wheels, v and u are the lateral and longitudinal velocities respectively, r is the yaw rate of the vehicle and a is the longitudinal distance between CG and front axle [49,50]. As expressed, the steering angle has a direct impact on slip angle, and subsequently, on lateral force. Now, revisiting the definition of toe angle, the variations of this angle means the same amount of changes in steering angle. Therefore, any changes in δ, other than steering input by driver, is undesired and is called the "steering error". A well designed suspension must minimize the variations of this angle, especially when the load is increasing on the wheel. For instance, when the suspension is under compression, toe changes should be as minimal as possible.

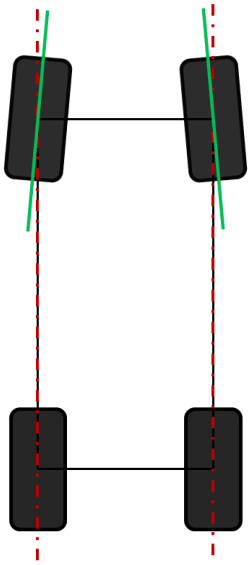

Figure 2- "Toe in" geometry

The other important characteristic of suspension is the variations of the camber angle. The camber angle is the angle between the vertical centerline of wheel and that of vehicle as viewed from the front plane. The camber angle also affects lateral forces; however, its effects are not as much as the toe angle. Figure 3 displays the DIN 70 000 definition of a positive camber along with the lateral force produced by camber variations [6]. Thus, very high alterations of this angle can cause steering error as well.

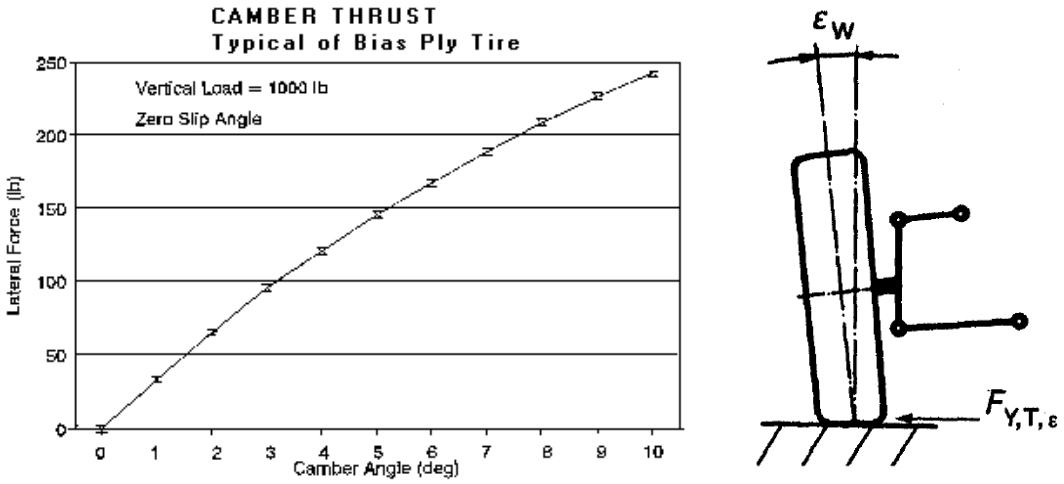

Figure 3- Camber angle and Camber thrust [6,51]

In regards to tire wear, minimizing the track alterations of a vehicle is essensial. Generally, the track is the width of an automobile between the centre of its wheels. The changes in a tires' contact patch in the global Y direction is known as track alteration, and it causes tire erosion. It also has a very slight impact on lateral forces which may cause problems. Therefore, it should be near zero while steering and during wheel travel. Figure 4 indicates the definition of front track, named as *w*.

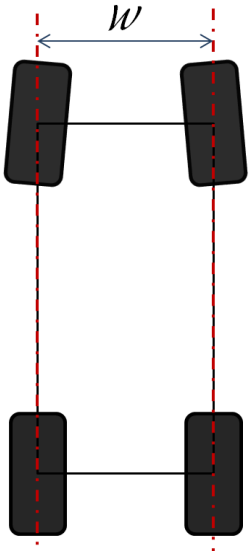

Figure 4- Track

There are some static characteristics that play a role in road holding. The scrub radius, which is defined based on the kingpin inclination angle of steering axis, shown in Figure 5, should not be zero. The reason lies in the role of the scrub radius in transferring the sense of the road to the driver. Also, a small amount of inclination angle can bring a better stability to the vehicle [1,6]. The kingpin inclination angle is the angle between the picture of steering axis on front plane and that of wheel's vertical axis.

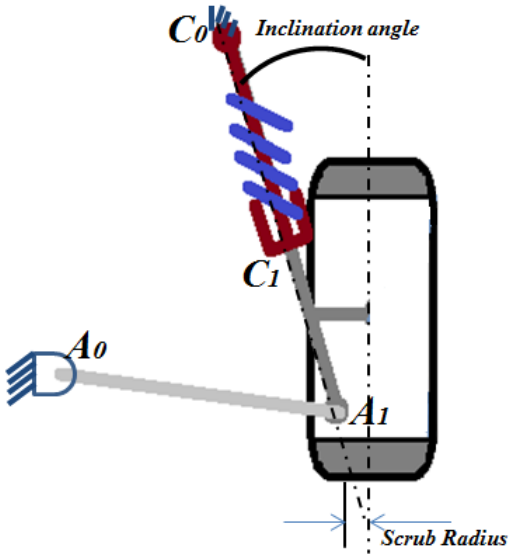

Figure 5- Kingpin inclination angle and Scrub radius

The caster angle is also important for vehicle stability. It has the same definition of inclination angle except that it refers to a side plane. Figure 5 indicates the definition of this angle regarding DIN 70 000 [6]. For better longitudinal stability, a small amount of caster angle, namely 0-5 degrees, is suggested [6,51].

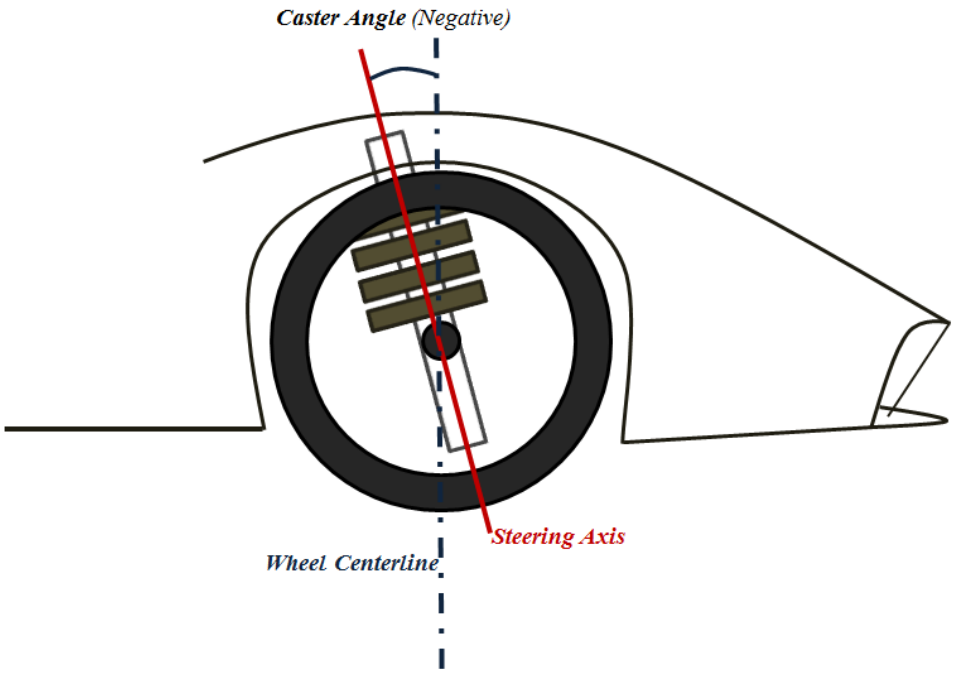

Figure 6- Negative Caster Angle

In front suspension systems, the lack of stability, tire erosion, and bump-steer are unwanted results of a poorly designed suspension. There have been many studies on the characteristics that play main roles in increasing stability and reliability of a suspension. Also, mechanisms that help prevent undesired movements of wheels had been designed, and they lead vehicles toward their optimum performance level. In the next section, these mechanisms will be discussed.

3.3 Suspension Mechanisms

As previously discussed, for better road holding, suspensions use mechanisms made of linkages. In this section, the most popular mechanisms are named, and a brief explanation is given. Then, a detailed modelling is provided for two of the widely used mechanisms in vehicle manufacturing, the MacPherson and the double-wishbone.

It is perhaps the case that the solid axle suspension was the very first suspension mechanism that was used by human beings during the era ox-driven carts. This suspension is also known as a dependent suspension, and nowadays, it benefits from modern leaf springs and coil springs to provide better comfort. Because of its heavy mass, it is rarely used as a front suspension, i.e. in heavy trucks. Also, for improving the road holding abilities of the suspension, it may be used with linkages such as a "Watt Mechanism", as shown in Figure 7 [1].

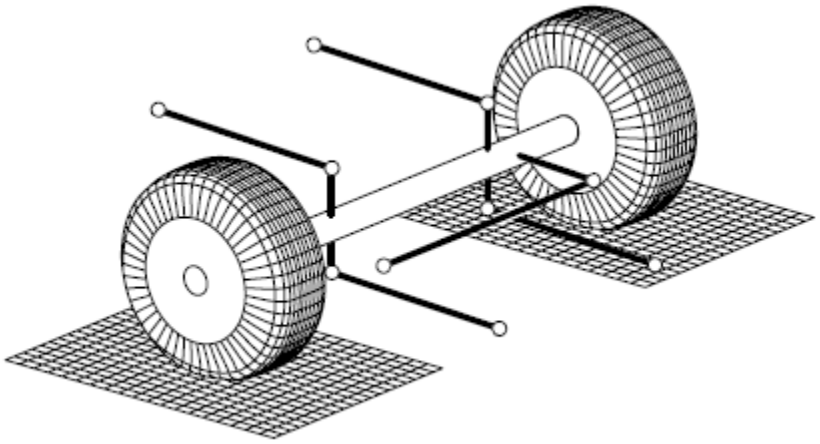

Figure 7- Solid axle suspension linked with Watt Mechanism [1]

The MacPherson, another type of suspension, is primarily used in smaller vehicles. This suspension is an independent suspension as the wheels of the same axle are held independently. Initially, the suspension was specifically designed for compact cars; however, it is now used in regular sized vehicles as well. It uses a coil spring and a shock absorber in its linkage system. The MacPherson suspension will be discussed in details further on this chapter. Figure 8 is a schematic of MacPherson suspension.

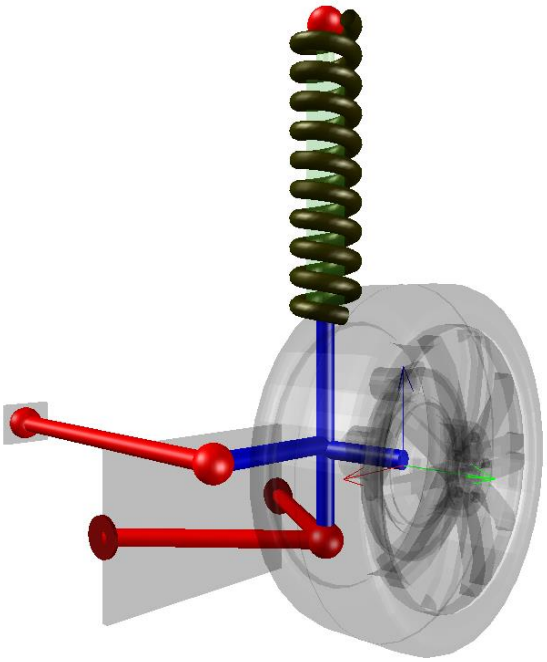

Figure 8- MacPherson schematic

Another independent suspension which is widely used in automotive manufacturing is the double-wishbone. This mechanism is also known as double-A arms and SLA (short-long arms). Due to its upper arm, it needs more space in global Y direction of the vehicle. On the other hand, the spring and damper is not a part of control mechanism and requires less space in global Z direction. Figure 9 indicates a typical double-wishbone suspension. In the following pages, this mechanism is studied in detail.

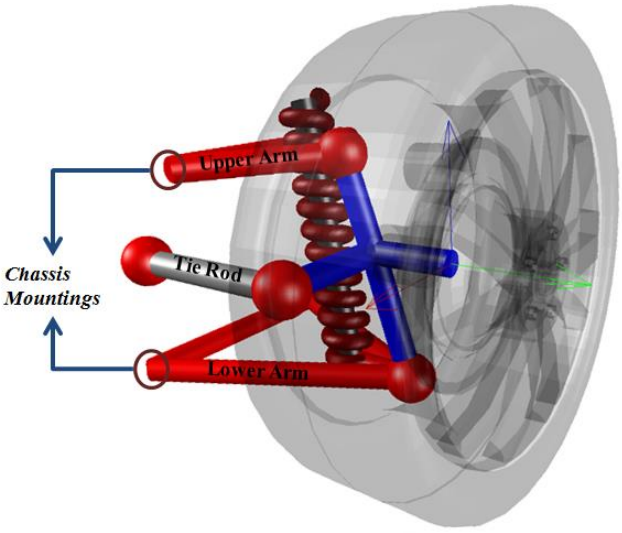

Figure 9- Double-wishbone schematic

The multi-link suspension is also an independent suspension that is mostly used in modern vehicles. In contrast to the MacPherson and the double-wishbone, replacing bushings with mechanical joints will result in no kinematical degrees of freedom. Therefore, the role of bushings is crucial in multi-link suspensions to provide dynamical degrees of freedom as forces are applied to the wheel. Figure 10 displays the rear axle of a manufactured electric car using multi-link suspension.

Figure 10- Mercedes-Benz SLS AMG Electric Drive rear axle[52]

3.4 MacPherson Suspension Modelling

In this section, a detailed study is done on the MacPherson suspension. One of the standard methods for analyzing a suspension with one or two kinematical degrees of freedom is to avoid bushings and consider mechanical joints with the same performance [17,21]. As shown in Figure 11, the MacPherson suspension is modelled in 3-dimensions by links and joints. The general calculation of the degrees of freedom of a system can be shown as:

$$\boldsymbol{DOF = n \times 6 - (m \times 5 + p \times 4 + q \times 3)} \qquad \textbf{(3-2)}$$

where n is the number of bodies, m is the number of revolute joints and prismatic joints, p is the number of universal joints, and q is the number of spherical joints. Regarding the MacPherson mechanism indicated in Figure 11, points D and E indicate revolute joints that connect the lower arm to chassis and operate in the same direction, which is equivalent to one revolute joint. Point B_0 shows a universal joint

which mounts the suspension to the steering rack. The steering rack itself is a body constrained to the chassis with a gear joint, which can be considered as a body jointed to the chassis with a prismatic joint, as is discussed in the next chapter. Points C_0 , A and B are spherical joints and point C is a prismatic joint. Counting the abovementioned mechanical joints indicate 1 revolute joint, 2 prismatic joints, 1 universal joint and 3 ball joints. Thus, the degrees of freedom can be achieved as follows:

$$DOF = 5 \times 6 - (3 \times 5 + 1 \times 4 + 3 \times 3) = 2 \qquad \textbf{(3-3)}$$

3.4.1 Equations

A schematic view of the MacPherson strut is provided in Figure 11. As shown, this suspension includes a lower arm, a spindle, a tie-rod and a strut. As mentioned in the DOF analysis, the chassis mounting points are named as D and E for the control arm and C_0 for the strut. B_0 is the connection of tie-rod to the steering mechanism. B, C and A are linkage connection points. Point P refers to the wheel's assembly position. Considering that A_0 is the orthogonal projection of $\overrightarrow{DA}$ on $\overrightarrow{DE}$, one can write the 3-D vector relations for a general MacPherson mechanism as below.

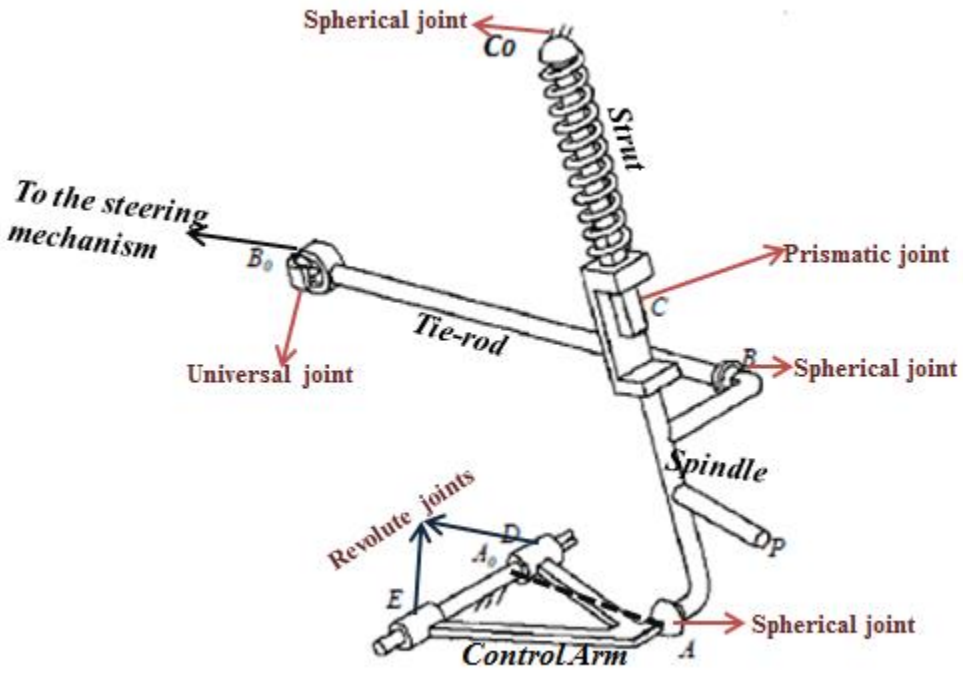

Figure 11-MacPherson Mechanism and its points' names [17]

$$\overrightarrow{\boldsymbol{A_0A}} + \overrightarrow{\boldsymbol{AC}} + \overrightarrow{\boldsymbol{CC_0}} + \overrightarrow{\boldsymbol{C_0A_0}} = \mathbf{0}$$
$$\overrightarrow{\boldsymbol{B_0B}} + \overrightarrow{\boldsymbol{BA}} + \overrightarrow{\boldsymbol{AA_0}} + \overrightarrow{\boldsymbol{A_0B_0}} = \mathbf{0} \quad \textbf{(3-4)}$$

The control arm is the lowest link in the MacPherson suspension mechanism. This link is connected to the chassis with revolute joints on points D and E as shown in Figure 11. The revolute joints allow the control arm to rotate along the direction of $\overrightarrow{DE}$. Point A, as shown in the figure, is located at the end of control arm. Therefore, in relation to the degrees of freedom of the control arm, it can only rotate about $\overrightarrow{DE}$. The vector of the rotation arm of point A along $\overrightarrow{DE}$ is $\overrightarrow{AA_0}$, where, as mentioned before, A_0 is found from the orthogonal projection of $\overrightarrow{DA}$ on $\overrightarrow{DE}$. Thus, the position of point A can be found by a rotation matrix, which is named $R_{ControlArm}$ in the following equations and expresses the rotation of the control arm along the direction of $\overrightarrow{DE}$. Now, let θ be the rotating angle of control arm from its initial position, A_1 the initial position of point A and $\boldsymbol{u}_{DE}$ the unit vector of $\overrightarrow{DE}$ direction:

$$\boldsymbol{u}_{DE} = \begin{bmatrix} u \\ v \\ w \end{bmatrix} = \frac{\overrightarrow{DE}}{|DE|} \quad \textbf{(3-5)}$$

Regarding the definition of A_0, this point will be found as:

$$A_0 = \boldsymbol{u}_{DE} \cdot \overrightarrow{DA_1} + D \quad \textbf{(3-6)}$$

Therefore, the following equation can express the position of point A, while rotation happens:

$$\begin{bmatrix} [A] \\ 1 \end{bmatrix}_{4\times1} = [R_{ControlArm}]_{4\times4} \times \begin{bmatrix} [A_1] \\ 1 \end{bmatrix}_{4\times1} \quad \textbf{(3-7)}$$

where, $[R_{ControlArm}]$ is a 4×4 matrix indicated below.

$$[R_{ControlArm}] = \begin{bmatrix} u^2 + (v^2 + w^2)\cos\theta & uv(1-\cos\theta) - w\sin\theta & uw(1-\cos\theta) + v\sin\theta & \left(x_{A_0}(v^2+w^2) - u\left(y_{A_0}v + z_{A_0}w\right)\right)(1-\cos\theta) + \left(y_{A_0}w - z_{A_0}v\right)\sin\theta \\ uv(1-\cos\theta) + w\sin\theta & v^2 + (u^2+w^2)\cos\theta & vw(1-\cos\theta) - u\sin\theta & \left(y_{A_0}(u^2+w^2) - v\left(x_{A_0}u + z_{A_0}w\right)\right)(1-\cos\theta) + \left(z_{A_0}u - x_{A_0}w\right)\sin\theta \\ uw(1-\cos\theta) - v\sin\theta & vw(1-\cos\theta) + u\sin\theta & w^2 + (u^2+v^2)\cos\theta & \left(z_{A_0}(u^2+v^2) - w\left(x_{A_0}u + y_{A_0}v\right)\right)(1-\cos\theta) + \left(x_{A_0}v - y_{A_0}u\right)\sin\theta \\ 0 & 0 & 0 & 1 \end{bmatrix}$$

(3-8)

Regarding the prismatic joint, whose location is represented by point C in Figure 11, the spindle and strut are constrained to have the same rotation in three-dimensional space. Therefore, the rotation matrix of the spindle, which represents the direction changes of vectors on the spindle, is the same as that of the strut. This rotation matrix should include rotations along global X,Y and Z axes, with extrinsic rotation angles of ϕ, ψ and γ, respectively. As the spindle is a rigid body, the length of any vector on the spindle should remain the same at any time. However, $\overrightarrow{CC_0}$, the vector which represents the geometry of the strut, does not have a constant length during a working cycle of mechanism. The aforementioned rotation matrix is defined in equation (3-9).

$$R_s = R_Z(\gamma) \times R_Y(\psi) \times R_X(\phi) \tag{3-9}$$

where R_Z, R_Y and R_X are rotation matrixes along Z,Y and X axes respectively and as follows.

$$\begin{cases} \boldsymbol{R_X(\phi)} = \begin{bmatrix} 1 & 0 & 0 & 0 \\ 0 & \cos\phi & -\sin\phi & 0 \\ 0 & \sin\phi & \cos\phi & 0 \\ 0 & 0 & 0 & 1 \end{bmatrix} \\ \boldsymbol{R_Y(\psi)} = \begin{bmatrix} \cos\psi & 0 & \sin\psi & 0 \\ 0 & 1 & 0 & 0 \\ -\sin\psi & 0 & \cos\psi & 0 \\ 0 & 0 & 0 & 1 \end{bmatrix} \\ \boldsymbol{R_Z(\gamma)} = \begin{bmatrix} \cos\gamma & -\sin\gamma & 0 & 0 \\ \sin\gamma & \cos\gamma & 0 & 0 \\ 0 & 0 & 1 & 0 \\ 0 & 0 & 0 & 1 \end{bmatrix} \end{cases} \tag{3-10}$$

Now, let A_1, C_1 and P_1 be the initial positions of points A, C and P respectively. Thus, relations (3-11) to (3-13) can be derived for the vectors on the spindle as follows:

$$\begin{bmatrix} \overrightarrow{AC} \\ 0 \end{bmatrix}_{4\times1} = [R_s]_{4\times4} \times \begin{bmatrix} \overrightarrow{A_1C_1} \\ 0 \end{bmatrix}_{4\times1} \tag{3-11}$$

$$\begin{bmatrix} \overrightarrow{BA} \\ 0 \end{bmatrix}_{4\times1} = [R_s]_{4\times4} \times \begin{bmatrix} \overrightarrow{C_1A_1} \\ 0 \end{bmatrix}_{4\times1} \tag{3-12}$$

$$\begin{bmatrix} \overrightarrow{AP} \\ 0 \end{bmatrix}_{4\times1} = [R_s]_{4\times4} \times \begin{bmatrix} \overrightarrow{A_1P_1} \\ 0 \end{bmatrix}_{4\times1} \tag{3-13}$$

To provide the equations of the strut, the unit vector of $\overrightarrow{C_1C_0}$ should be found from equation (3-14) and used in equation (3-15) to express the changes of the struts direction.

$$\boldsymbol{u}_{C_1C_0} = \frac{\overrightarrow{C_1C_0}}{|C_1C_0|} \tag{3-14}$$

$$\begin{bmatrix} \boldsymbol{u}_{CC_0} \\ 0 \end{bmatrix}_{4\times1} = [R_s]_{4\times4} \times \begin{bmatrix} \boldsymbol{u}_{C_1C_0} \\ 0 \end{bmatrix}_{4\times1} \tag{3-15}$$

Considering L_{CC_0} as the length of strut, relation (3-16) indicate the geometry of strut:

$$\overrightarrow{CC_0} = L_{CC_0} \times \boldsymbol{u}_{CC_0} \tag{3-16}$$

Regarding Figure 11, the tie-rod, which is the connecting rod between the suspension and steering mechanisms, can be represented by $\overrightarrow{B_0B}$. The tie-rod cannot rotate along its own axis and has always a constant length. Thus, by using the former defined 3-Dimensional rotation matrix in equations (3-9) and (3-10), and assuming that C_1 is the initial position of the point C, one can derive required algebraic equations of tie-rod's position as below.

$$\begin{gathered} \begin{bmatrix} [\overrightarrow{B_0B}] \\ 0 \end{bmatrix}_{4\times1} = [R_{TieRod}]_{4\times4} \times \begin{bmatrix} [\overrightarrow{B_0B_1}] \\ 0 \end{bmatrix}_{4\times1} \\ R_{TieRod} = R_Z(\eta) \times R_Y(\beta) \times R_X(\alpha) \end{gathered} \tag{3-17}$$

where R_{TieRod} is the rotation matrix of the tie-rod. The universal joint will also require rotational constraint. As it cannot rotate along its axis, equation (3-18) expresses this rotational constraint.

$$\begin{bmatrix} \alpha \\ \beta \\ \eta \end{bmatrix} \cdot \left(\overrightarrow{B_0B}\right) = 0 \tag{3-18}$$

Now, let's name the contact point of tire and the road point T and its initial position T_1. The following equation will then expresses the wheel travel concept in the suspension.

$$\begin{gathered} \Delta z_{wheel} + z_{T_1} = z_T \\ z_T = z_A - z_{AT} \end{gathered} \tag{3-19}$$

In the above equation, *z* refers to the vertical component of the points, AT is a vector on the spindle and between points *A* and T.

3.4.2 Steering Connection

Steering is also an input into the suspension system. As mentioned, B_0 is the connecting point between the rack and the spindle. When steering is applied, there actually is a movement in Y direction at B_0. Therefore, one can consider the effect of steering by adding another equation of motion on this point, instead of fixing it to the body. Thus, equations (3-20) and (3-21) can be considered as another driver equation along with all other above equations.

$$y_{B_0} = \left(y_{B_0}\right)_0 + \Delta y_{Rack} \tag{3-20}$$

$$\xrightarrow{yields} \quad B_0 = \begin{bmatrix} x_{B_0} \\ \left(y_{B_0}\right)_0 + \Delta y_{Rack} \\ z_{B_0} \end{bmatrix} \tag{3-21}$$

Term $\left(y_{B_0}\right)_0$ indicates the initial position of B_0 in Y direction of the global coordinate.

Now, the model yields the suspension movements while both steering and wheel travel is applied. The sets of equations and unknowns are illustrated in equation (3-22), where $\boldsymbol{q}$ is the vector of variables and $\boldsymbol{\Phi}$ is the constraints.

$$\boldsymbol{q} = \begin{bmatrix} \phi \\ \gamma \\ \psi \\ \alpha \\ \beta \\ \eta \\ \theta \\ L_{CC_0} \end{bmatrix}$$

$$\boldsymbol{\Phi} = \begin{bmatrix} [R_{ControlArm}]_{4\times4} \times \begin{bmatrix} [A_1] \\ 1 \end{bmatrix}_{4\times1} - \begin{bmatrix} [A_0] \\ 1 \end{bmatrix}_{4\times1} + [R_s]_{4\times4} \times \begin{bmatrix} \overrightarrow{A_1C_1} \\ 0 \end{bmatrix}_{4\times1} + L_{CC_0} \times [R_s]_{4\times4} \times \begin{bmatrix} u_{C_1C_0} \\ 0 \end{bmatrix}_{4\times1} + \begin{bmatrix} \overrightarrow{C_0A_0} \\ 0 \end{bmatrix}_{4\times1} \\ [R_{ControlArm}]_{4\times4} \times \begin{bmatrix} [A_1] \\ 1 \end{bmatrix}_{4\times1} - \begin{bmatrix} [A_0] \\ 1 \end{bmatrix}_{4\times1} + [R_s]_{4\times4} \times \begin{bmatrix} \overrightarrow{B_1A_1} \\ 0 \end{bmatrix}_{4\times1} + [R_{TieRod}]_{4\times4} \times \begin{bmatrix} \overrightarrow{[B_0B_1]} \\ 0 \end{bmatrix}_{4\times1} + \begin{bmatrix} \overrightarrow{A_0B_0} \\ 0 \end{bmatrix}_{4\times1} \\ \begin{bmatrix} \alpha \\ \beta \\ \eta \end{bmatrix} \cdot \left(\overrightarrow{B_0B}\right) = 0 \\ z_T = z_A - z_{AT} \\ y_{B_0} - \left(y_{B_0}\right)_0 - \Delta y_{Rack} \end{bmatrix} \tag{3-22}$$

3.4.3 Modelling Verification

As the equations are based on a new method that combines both vector analyses and rotation matrices, the results of the modelling should be verified by multi-body dynamics software. In this section, the ADAMS software is used.

Verification of a real suspension is provided by comparing the results of above equations solved by MATLAB and the suspension model in the ADAMS view. In the ADAMS model, bushings are avoided to focus on equation verification. Results shown are for the rotation angles of the spindle along the X, Y and Z axes. Rotation along X and Z are camber and toe respectively.

As is demonstrated in the plots of Figure 12, the results are exactly the same. Thus, the new method is perfectly accurate, and it yields only 8 equations.

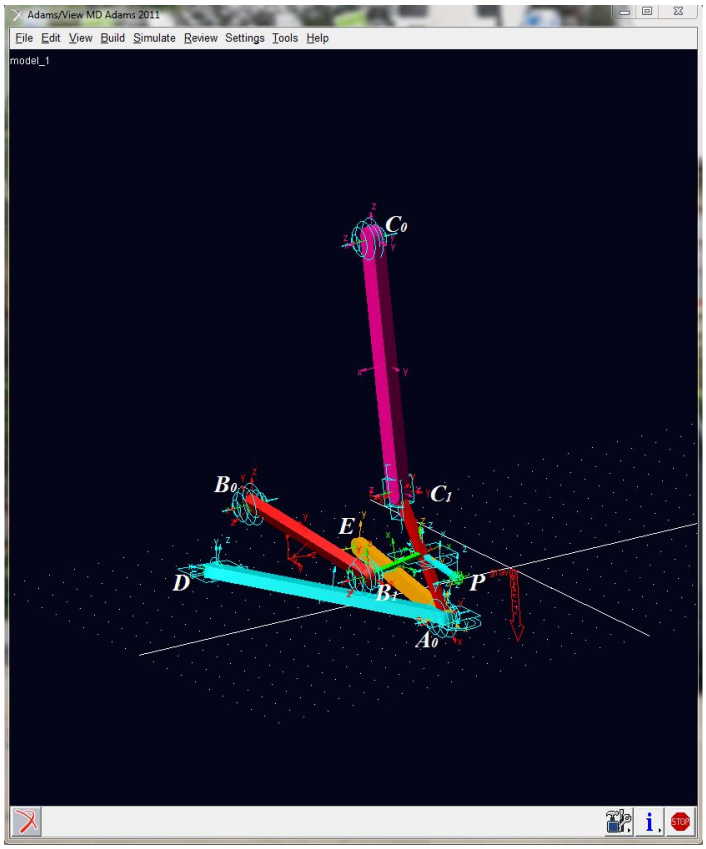

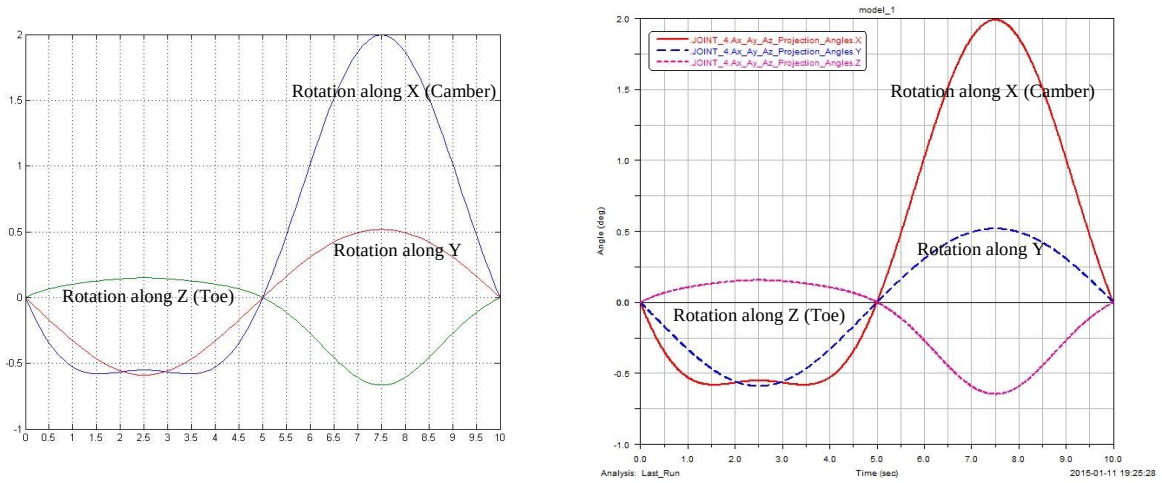

Figure 12- The Model in ADAMS View and results comparison in Matlab, left, and ADAMS, right

3.5 Double-Wishbone Suspension Modelling

As formerly mentioned in the MacPherson analysis, one standard method of analyzing a suspension with one or two kinematical degrees of freedom is to avoid bushings and consider mechanical joints with the same performance. Figure 13, shows a schematic 3D double-wishbone suspension. Considering the same explanations about tie-rod, steering system and control arm in the MacPherson mechanism, the number of the joints can be found. Points A, B and C indicate spherical joints, couple points D and E, and F and G express two independent revolute joints for lower and upper wishbones respectively, and B_0 indicates a universal joints that connects the suspension to the steering system and explained before. According to Equation (3-2) and by considering 2 revolute joints, 3 spherical joints, 1 universal and 1 prismatic joint, the double-wishbone suspension will have 2 degrees of freedom.

3.5.1 Equations

A schematic view of the double-wishbone is provided in Figure 13. As shown, this suspension includes a lower-arm, a spindle, a tie-rod, and an upper-arm. To make the understanding easier, name of hard points are the same as in the MacPherson system. For instance, the chassis mounting points are named as D and E for lower arm, B_0 is the connection of the tie-rod to the steering mechanism, and B, C and A are linkage connection points. The difference being that C_0 for this system is the orthogonal projection of $\overrightarrow{FC}$ on $\overrightarrow{FG}$.

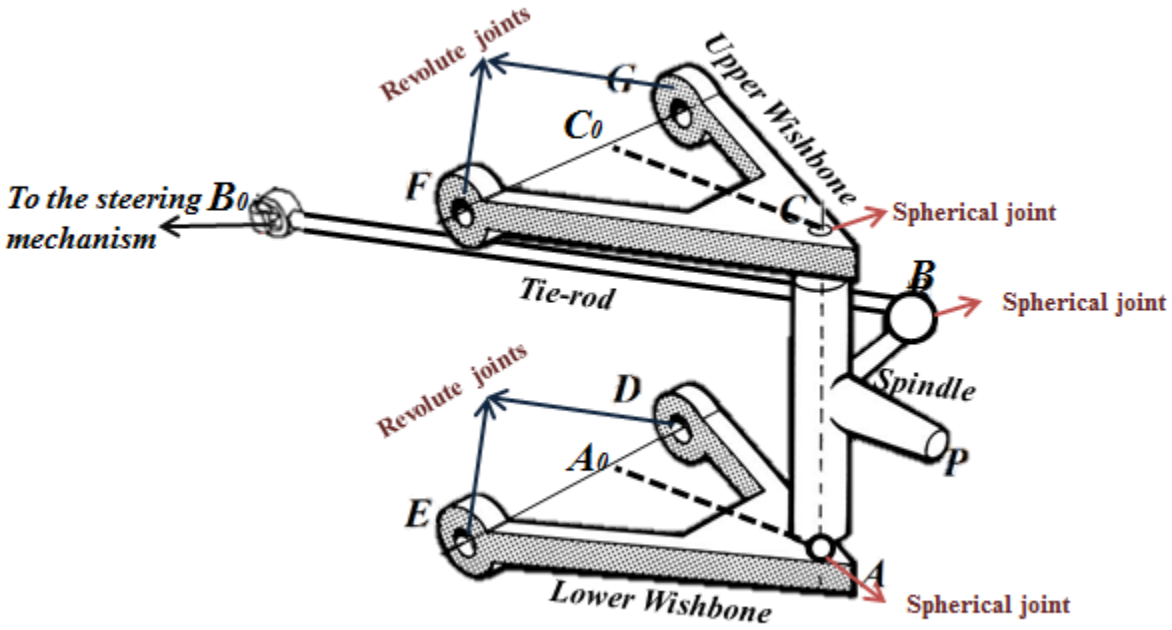

Figure 13-Double-wishbone schematic geometry [53]

Having these names allow for the usage of exactly the same equations (3-2) and (3-3) for the needed vector geometry.

The lower arm is the lowest link in the double-wishbone, which is exactly the same as in the MacPherson. This link is connected to the chassis with revolute joints on points D and E, as shown in Figure 13. The revolute joints only allow a rotation along the direction of $\overrightarrow{DE}$. Therefore, the equations that express the lower wishbone's movements are equations (3-5) to (3-8). Also, the upper-arm, the highest link in double-wishbone mechanism, can only rotate along the same direction as lower arm. However, it is connected to the chassis at point F, and its amount of rotation is different from the lower arm, indicated as ζ in the following equations. In this case, one can define C_0, the orthogonal projection of FC on its pivoting axis, using DE direction and equation (3-5) as follow.

$$\xrightarrow{(3-4)} \quad C_0 = \boldsymbol{u}_{DE} \cdot \overrightarrow{FA_1} + F \qquad \textbf{(3-23)}$$

Now, letting C_1 be the initial position of point C, equation (3-24) will express the position of point C.

$$\begin{bmatrix}[C]\\1\end{bmatrix}_{4\times1} = [R_{UpperArm}]_{4\times4} \times \begin{bmatrix}[C_1]\\1\end{bmatrix}_{4\times1} \quad \textbf{(3-24)}$$

where $[R_{UpperArm}]$ is found as follow.

$$[R_{UpperArm}] = \begin{bmatrix} u^2+(v^2+w^2)\cos\zeta & uv(1-\cos\zeta)-w\sin\zeta & uw(1-\cos\zeta)+v\sin\zeta & \left(x_{C_0}(v^2+w^2)-u\left(y_{C_0}v+z_{C_0}w\right)\right)(1-\cos\zeta)+\left(y_{C_0}w-z_{C_0}v\right)\sin\zeta \\ uv(1-\cos\zeta)+w\sin\zeta & v^2+(u^2+w^2)\cos\zeta & vw(1-\cos\zeta)-u\sin\zeta & \left(y_{C_0}(u^2+w^2)-v\left(x_{C_0}u+z_{C_0}w\right)\right)(1-\cos\zeta)+\left(z_{C_0}u-x_{C_0}w\right)\sin\zeta \\ uw(1-\cos\zeta)-v\sin\zeta & vw(1-\cos\zeta)+u\sin\zeta & w^2+(u^2+v^2)\cos\zeta & \left(z_{C_0}(u^2+v^2)-w\left(x_{C_0}u+y_{C_0}v\right)\right)(1-\cos\zeta)+\left(x_{C_0}v-y_{C_0}u\right)\sin\zeta \\ 0 & 0 & 0 & 1 \end{bmatrix}$$

(3-25)

Now, if extrinsic rotation angles along the global X,Y and Z axes, are named as ϕ, ψ and γ, respectively, then the equations of the spindle will be defined by equations (3-9) to (3-13).

Regarding Figure 13, the tie-rod, which is the connecting rod between suspension and steering mechanism, is the $\overrightarrow{B_0B}$ vector. The behavior of the tie-rod in the double-wishbone suspension is exactly the same as in the MacPherson. Therefore, if α, β and η are the extrinsic rotation angles of the tie-rod, equations (3-17) and (3-18) will represent the behavior of this link.

As the inputs are also the same as in any other suspension, steering input and wheel travel can be represented via equations (3-19) and (3-20). All in all,$\boldsymbol{\Phi}$ and $\boldsymbol{q}$ define the sets of equations and variables for the double-wishbone would be as follows.

$$\boldsymbol{q} = \begin{bmatrix}\phi\\ \gamma\\ \psi\\ \alpha\\ \beta\\ \eta\\ \theta\\ \zeta\end{bmatrix} \quad \textbf{(3-26)}$$

$\boldsymbol{\Phi}$

$$= \begin{bmatrix} [R_{ControlArm}]_{4\times4} \times \begin{bmatrix}[A_1]\\1\end{bmatrix}_{4\times1} - \begin{bmatrix}[A_0]\\1\end{bmatrix}_{4\times1} + [R_s]_{4\times4} \times \begin{bmatrix}\overrightarrow{A_1C_1}\\0\end{bmatrix}_{4\times1} - [R_{UpperArm}]_{4\times4} \times \begin{bmatrix}[C_1]\\1\end{bmatrix}_{4\times1} + \begin{bmatrix}[C_0]\\1\end{bmatrix}_{4\times1} + \begin{bmatrix}\overrightarrow{A_0C_0}\\0\end{bmatrix}_{4\times1} \\ [R_{ControlArm}]_{4\times4} \times \begin{bmatrix}[A_1]\\1\end{bmatrix}_{4\times1} - \begin{bmatrix}[A_0]\\1\end{bmatrix}_{4\times1} + [R_s]_{4\times4} \times \begin{bmatrix}\overrightarrow{B_1A_1}\\0\end{bmatrix}_{4\times1} + [R_{TieRod}]_{4\times4} \times \begin{bmatrix}[\overrightarrow{B_0B_1}]\\0\end{bmatrix}_{4\times1} + \begin{bmatrix}\overrightarrow{A_0B_0}\\0\end{bmatrix}_{4\times1} \\ \begin{bmatrix}\alpha\\\beta\\\eta\end{bmatrix} \cdot \left(\overrightarrow{B_0B}\right) = 0 \\ z_T = z_A - z_{AT} \\ y_{B_0} - \left(y_{B_0}\right)_0 - \Delta y_{Rack} \end{bmatrix}$$

3.5.2 Modelling Verification

To make sure this method also works with other multi-body dynamics software, verification is done by MapleSim software, which verifies using the graph theory method. Figure 14 indicates the model in MapleSim software, and Figure 15 and Figure 16 represent a comparison between the results of the modelled equations in Matlab and MapleSim.

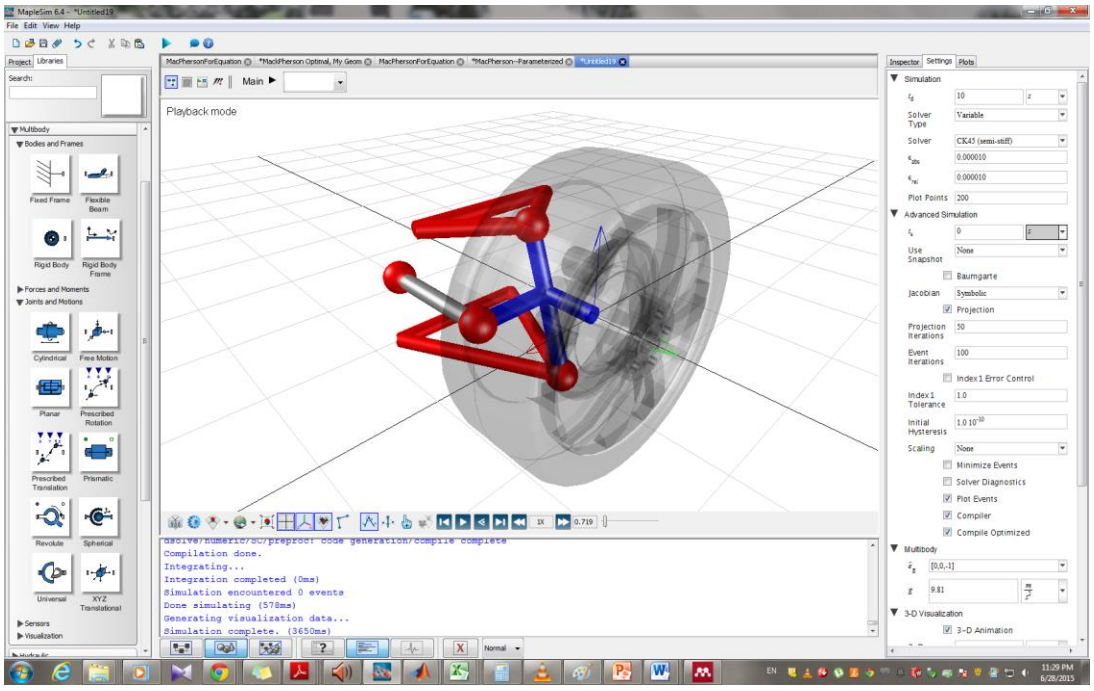

Figure 14- Double-wishbone model in MapleSim

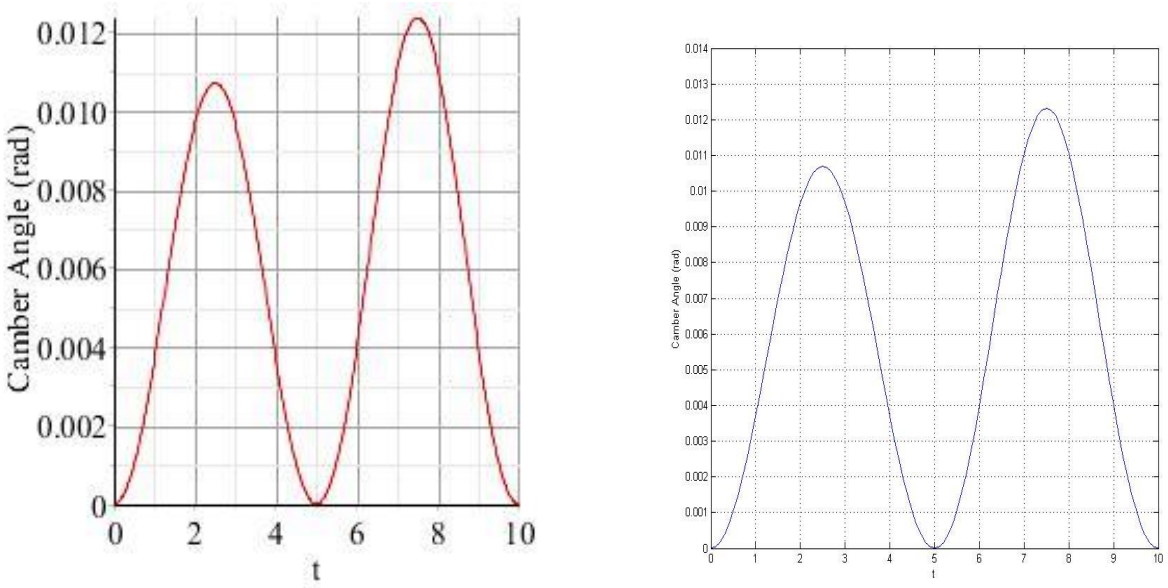

Figure 15- Camber Angle in MapleSim and MATLAB

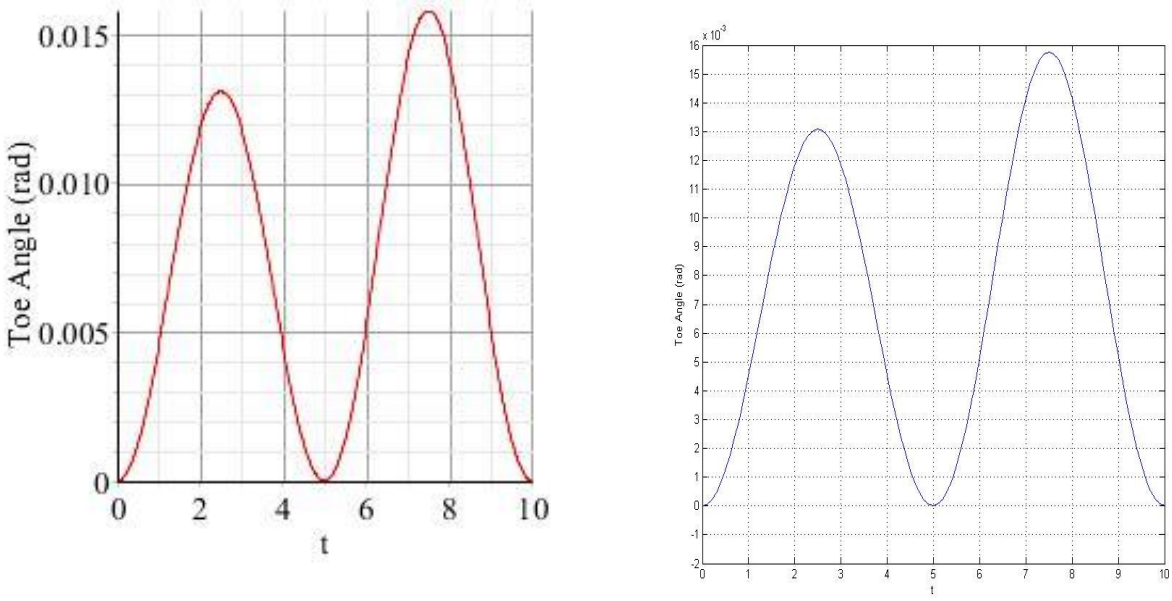

Figure 16- Toe Angle in MapleSim and Matlab

3.6 Anti-roll bar

The anti-roll bar is a torsional bar that connects the suspensions of each side together and reduces the amount of roll of the body during cornering. It is usually fixed to the lower arm and to the chassis with some bushings. In Figure 17 and Figure 18, a schematic of an anti-roll bar is shown. As the body rolls during cornering, the distance between the wheels and the body alters at each side. This change would be the same in amount but opposite in the direction. Therefore, by the solving the same wheel travel equations, the displacement of the anti-roll bar mounting points to the suspension would be found. With the displacement, one can use Z component and the effective length of the anti-roll bar, named $l_{effective}$ in equation (3-28), to find the torsion angle of anti-roll bar while a known amount of body roll is applied. Considering the amount of body roll is ϕ_{Body} , the resulted anti-roll bar torsion is $\theta_{anti-roll\ bar}$ and the vehicles track is W, equation (3-27) yields the relation between the body roll and wheel travel, which consequently results in finding the torsion of anti-roll bar by equation (3-28).

$$\sin(\phi_{Body}) = \frac{2\Delta z_{wheel}}{W} \quad \textbf{(3-27)}$$

$$\Delta z_{wheel} \xrightarrow{solving\ the\ system\ equations} \Delta z_{l-arb}\ \&\ \Delta z_{r-arb}$$

$$\arcsin\left(\frac{\Delta z_{l-arb} + \Delta z_{r-arb}}{l_{effective}}\right) = \theta_{anti-roll\ bar} \quad \textbf{(3-28)}$$

In the above equations, Δz_{l-arb} is the displacement of anti-roll bar's connecting point to the left suspension in Z direction and Δz_{r-arb} is the displacement of anti-roll bar's connecting point to the right suspension in Z direction. Therefore, the motion ratio will be:

$$MR = \frac{d(\theta_{anti-roll\ bar})}{d(\phi_{body})} \quad \textbf{(3-29)}$$

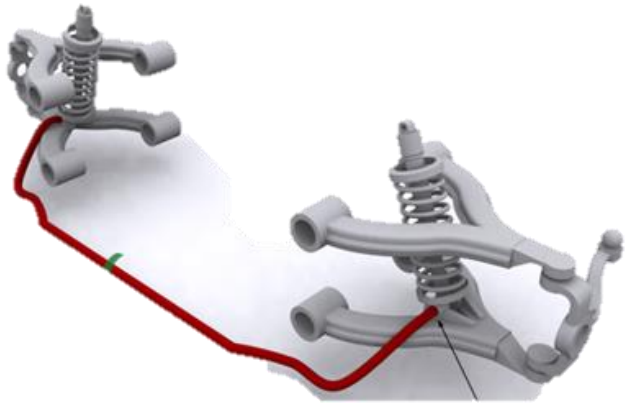

Figure 17- Anti-roll bar connection to double-wishbone suspension [54]

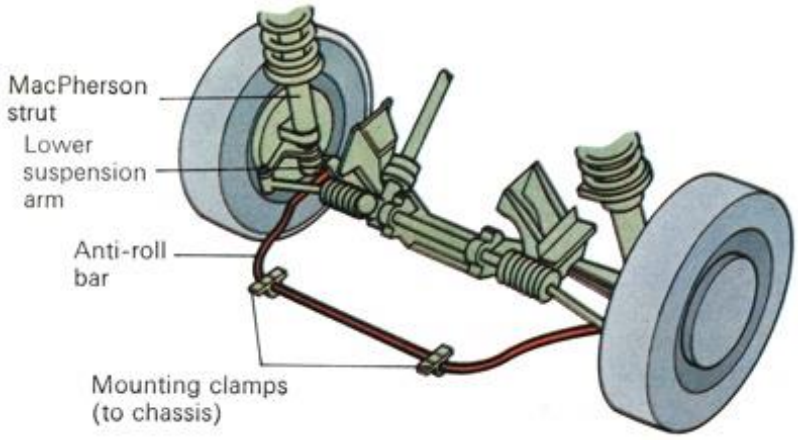

Figure 18-Anti-roll bar and MacPherson schematic [55]

Now that all the equations are written, by solving the system, all required suspension characteristics and sizing factors can be found. In terms of system characteristics, the scrub radius and the inclination angle are both static, and there is no need to find them by solving the system. However, toe, camber, and track alternations are three important characteristics that should be found during wheel travel and in different steering angles. Following relations yield system characteristics in relation to the equations of the system.

$$Camber\ Angle = \phi \quad \textbf{(3-30)}$$

$$Toe\ Angle = \gamma \quad \textbf{(3-31)}$$

$$Track\ Alterations = y_T - y_{T_1} \quad \textbf{(3-32)}$$

Chapter 4
Steering System

4.1 Introduction

The steering system is used for guiding the vehicle. The driver's applied motion is translated into angles applied on the wheels by steering system [56]. The steering system must be "robust, sensitive, and precise enough to inform the driver as comprehensively as possible about the various vehicle condition parameters and any alterations in these parameters" [1]. A similar explanation has been stated in other handbooks [56,57]. Regarding the goal of the steering system, it is very important that the steering wheel's angle and the steering angle on wheels correlate accurately and only small amounts of "play" are allowed in transferring the torque of steering wheel into the force on the vehicle's wheels. Although the purpose of the steering system is to provide desired angles for cornering, the driver is also receiving information about the steering system by feeling the required torque for desired steering angles. Therefore, no unwanted forces, i.e. friction, should affect the transmission of these forces to save the system's efficacy [58].

Amongst all the mechanisms for transferring the desired steering angles on the steerable wheels, rack and pinion mechanisms are the most widely used. Rack and pinion steering systems are used on every class and size of vehicle; from mid-sized family cars like Opel Astra 1997 and Peugeot 405, to faster and more luxury vehicles, such as the Audi A8 and Mercedes E and S Class, and it is also used in many light-weight vans. Some of the advantages of this mechanism over other steering mechanisms include its simplicity, having a play free and robust gear contact between rack and pinion [1], and its capability to be combined with all kinds of power assists.

Besides the type and robustness of a steering system, these mechanisms should also be able to provide a reasonable proportion between the inner and outer turn wheels to satisfy turning dynamics. After many years of using carts, Georg Lankensperger, a German carriage builder, created a type of steering geometry to solve the steering issue in 1817, which was later patented by his agent in England, Rudolph Ackermann, for horse-drawn carriages. This steering geometry is known as Ackermann steering. Later, tires were found subjects to affect steering performance and anti-Ackermann steering approaches were introduced to maximize racing car cornering performances. In this chapter, steering principles are going to be studied, along with a rack and pinion steering mechanism analysis [57].

4.2 Technology

There are many mechanisms that can transfer driver's steering input into a steering angle on wheels. Parallelogram and rack and pinion are the two main mechanisms for the aforementioned purposes. Parallelogram mechanism is based on a four-bar linkage that has two parallel and equal arms with a long coupler in the middle. It is also known as the Pitman-bar steering.

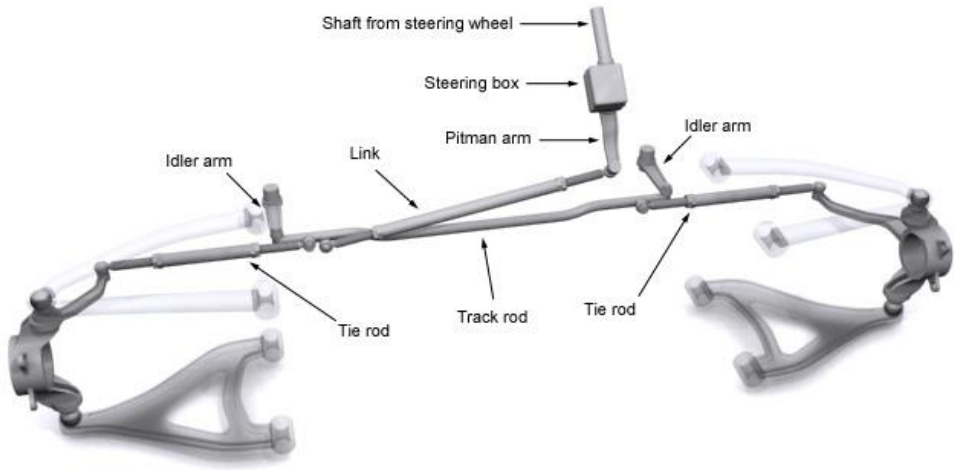

Figure 19-Parallelogram steering [54]

On the other hand, the rack and pinion mechanism is one of the widely used steering systems in the vehicle industry that uses gears for transferring the rotational input of the driver to a translational movement that causes steering on wheels, shown in Figure 25. The rack is a linear gear bar which is connected on each side to another bar, the tie-rod, with a universal joint. The other end of the tie-rods are connect to the spindles of the steerable suspensions of each side by spherical joints, and this connection helps the whole suspension-steering mechanism to output the desired steering angles onto the wheels. The focus of this thesis is on the rack and pinion mechanism and a detailed explanation is provided in following sections.

4.2.1 Modeling and Analysis

4.2.1.1 No assist

The steering column is a part of the steering mechanism that has the duty of transferring the steering input by the driver to the pinion. The forces on the rack can be dynamically modelled as shown in Figure 20.

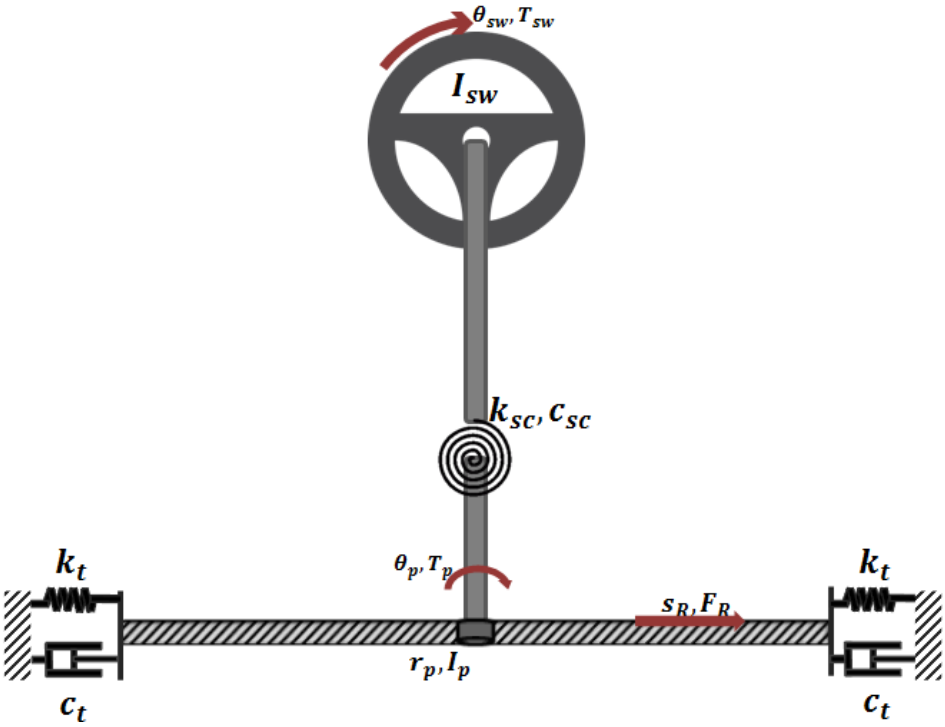

Figure 20- Schematic of rack and pinion model

Regarding this simplified model of the steering column, if the driver input is an angle into the steering wheel, one can write its dynamical equations as below.

$$k_{sc}(\theta_{sw} - \theta_p) + c_{sc}(\dot{\theta}_{sw} - \dot{\theta}_p) = I_p\ddot{\theta}_p + T_p \qquad \textbf{(4-1)}$$

where, and as shown in Figure 20, θ_{sw} is the rotation of the steering wheel, which is considered to be the input by driver, θ_p is the rotation of the pinion, I_p is the pinion's moment of inertia along its rotating axis, and T_p is the resisting torque on the pinion caused by the forces on the rack mostly due to resistance of the tires. The state space equations of the above equation would be as follows.

$$\begin{bmatrix}\dot{\theta}_p\\ \ddot{\theta}_p\end{bmatrix}=\begin{bmatrix}0 & 1\\ -\frac{k_{sc}}{I_p} & -\frac{c_{sc}}{I_p}\end{bmatrix}\begin{bmatrix}\theta_p\\ \dot{\theta}_p\end{bmatrix}+\begin{bmatrix}0 & 0\\ \frac{k_{sc}}{I_p} & \frac{c_{sc}}{I_p}\end{bmatrix}\begin{bmatrix}\theta_{sw}\\ \dot{\theta}_{sw}\end{bmatrix}+\begin{bmatrix}0\\ 1\end{bmatrix}T_p \qquad \textbf{(4-2)}$$

Considering that the steering gearbox is ideal and its efficiency is 100%, the relation between resisting torque on the pinion and resisting force on the rack can be found by a simple gear analysis as below.

$$\begin{gathered}P_p = P_R\\ \overrightarrow{T_p}.\dot{\vec{\theta}}_p = \overrightarrow{F_R}.\dot{\vec{s}}_R\\ \dot{\vec{\theta}}_p \times \overrightarrow{r_p} = \dot{\vec{s}}_R \overset{\dot{\vec{\theta}}_p \cdot \overrightarrow{r_p}}{\Longrightarrow} \dot{\theta}_p r_p = \dot{s}_R\\ T_p = F_R r_p\end{gathered} \qquad \textbf{(4-3)}$$

where P refers to the transferred power from the pinion to the rack, F_R is the transmitted force to the rack and s_R stands for the displacements of the rack.

In linear models, resistant forces produced by tires while steering can be simplified as an equivalent spring and damper forces, which resist linearly against rack movement. Therefore,

$$F_R = 2(K_t s_R + C_t \dot{s}_R) \qquad \textbf{(4-4)}$$

And by equations (4-2) to (4-4), the state space equation can be written as below.

$$\begin{bmatrix}\dot{\theta}_p\\ \ddot{\theta}_p\end{bmatrix}=\begin{bmatrix}0 & 1\\ -\frac{k_{sc}}{I_p}-2K_t r_p^2 & -\frac{c_{sc}}{I_p}-2C_t r_p^2\end{bmatrix}\begin{bmatrix}\theta_p\\ \dot{\theta}_p\end{bmatrix}+\begin{bmatrix}0 & 0\\ \frac{k_{sc}}{I_p} & \frac{c_{sc}}{I_p}\end{bmatrix}\begin{bmatrix}\theta_{sw}\\ \dot{\theta}_{sw}\end{bmatrix} \qquad \textbf{(4-5)}$$

As all the assists being used in steering systems try to reduce the applied torque by the driver, the required torque needs to be found. Equation (4-6) shows the relation between the input angle and the required torque while there are no assists.

$$T_{sw} - I_{sw}\ddot{\theta}_{sw} = k_{sc}(\theta_{sw} - \theta_p) + c_{sc}(\dot{\theta}_{sw} - \dot{\theta}_p) \qquad \textbf{(4-6)}$$

4.2.1.2 Hydraulic Assist

Here, in Figure 21, a real cooperation between the hydraulic system and rack and pinion is shown. This figure also indicates that the driver needs only rotate a hydraulic valve. That means that the main force for the translational movement of the rack is supplied by the hydraulic system. Then, by the movement of the rack, the pinion would rotate and after reaching the required position, the valve would be closed.

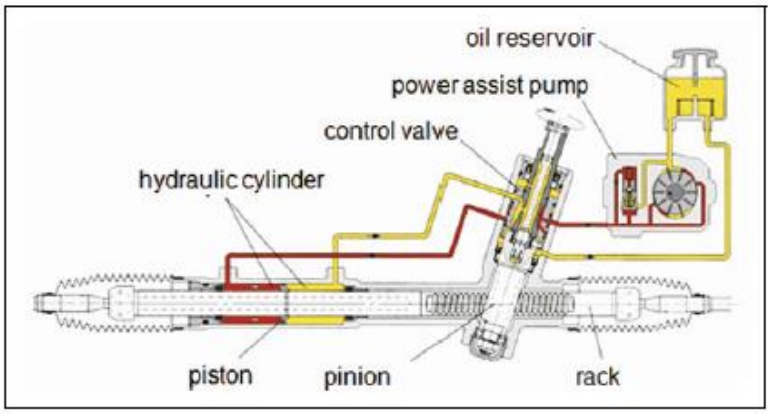

Figure 21-Hydraulic powered rack and pinion system [58]

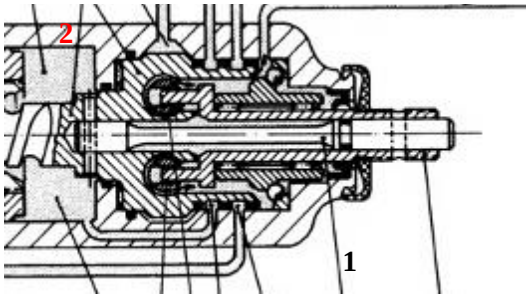

Figure 22- Torsional bar of hydraulic valve [56]

The rotary valve being used in the hydraulic system has a flexible torsional bar that connects the end of the steering column to the pinion, shown in Figure 22 as number 1. This torsional bar is the inner part of the rotary valve. As shown as number 2 in the same figure, the valve's housing is also connected to the steering gear. Therefore, when a steering angle is applied to the steering wheel by driver, and there is a resisting torque on the pinion, which was previously discussed, the torsion in the flexible bar causes the angle difference between the inside of the valve and the housing. This difference opens the hydraulic flow into the hydraulic cylinder and toward the required direction. The cylinder applies a great amount of force

into the rack and assists the driver for a more comfortable steering experience [56,58]. The block diagram of this mechanism is shown in Figure 23.

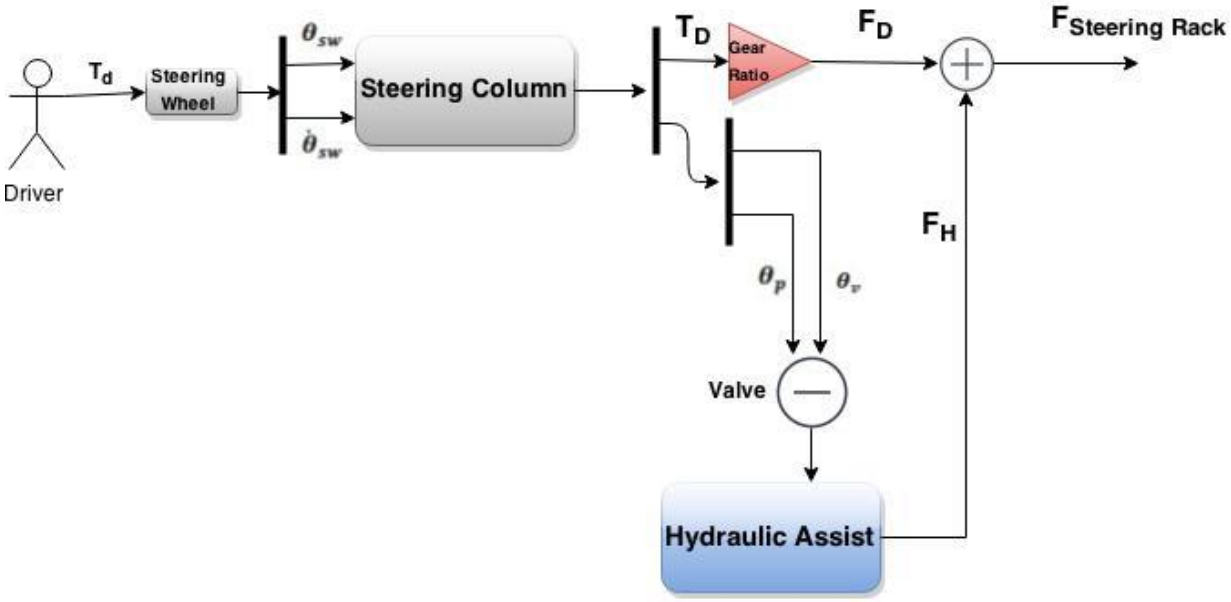

Figure 23-Hydraulic assisted steering block diagram

Knowing how the rotary valve works, one can model a rotary valve like a pilot-valve due to the fact that both valves could be modeled with four spool valves in a Whetstone's bridge connection [59]. According to Ogata [60], the linearized model of a servo-hydraulic system with a pilot-valve near its operating point yields the force produced by the hydraulic cylinder as follows.

$$F_H = \frac{A}{k_2}(k_1 x - A\rho\dot{y}) \qquad \textbf{(4-7)}$$

where, A is the area of cylinder's piston, ρ is the density of the hydraulic fluid, x is the input of the valve, $\dot{y}$ is the velocity of the piston, and k_1 and k_2 are the characteristic coefficients of valve and hydraulic cooperation that are dependent on ρ, gravity acceleration and the pressure of the hydraulic pump. As here, the input is the angle differential caused by torsional bar, and the piston movement is the same as rack movement, the above equation would yield the following relation between hydraulic assist force and steering column angles. The angles and mechanisms are schematically shown in Figure 24.

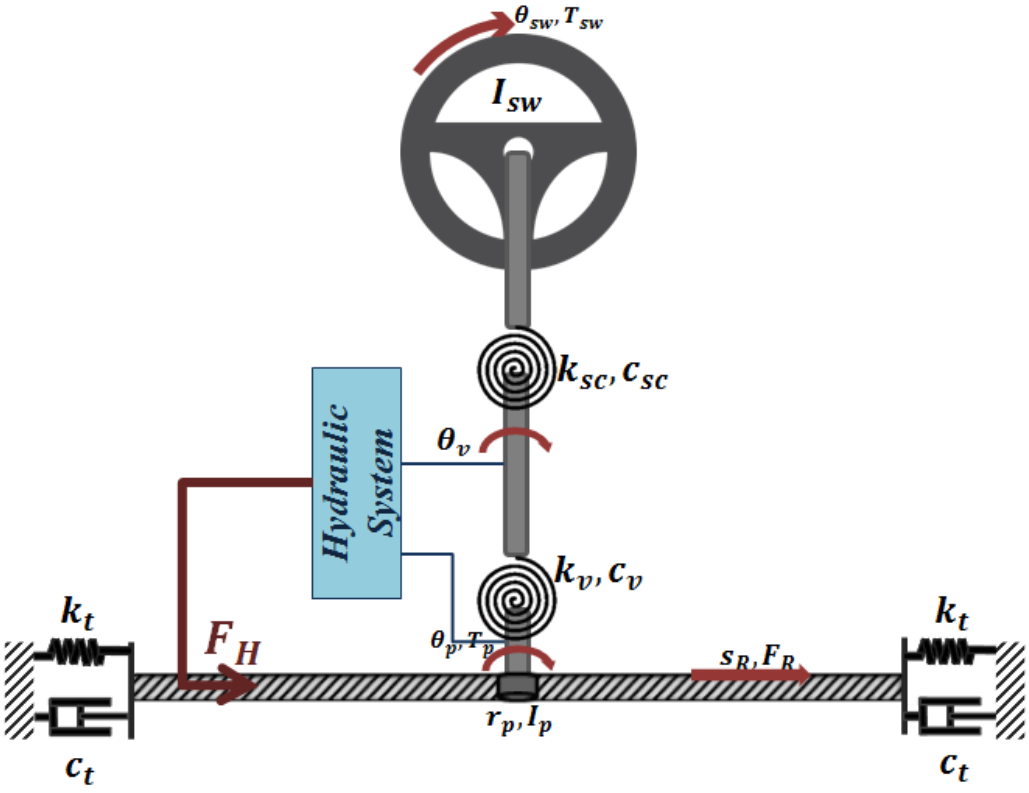

Figure 24- Schematic of hydraulic assisted rack and pinion

$$F_H = \frac{A}{k_2}\left(k_1(\theta_v - \theta_p) - A\rho r_p \dot{\theta}_p\right) \quad \textbf{(4-8)}$$

Note that in the above equation, the operating point is when $\theta_v - \theta_p$ is zero, as the hydraulic assist attempts to move and apply the force immediately. Therefore, the variables are correctly replaced. Regarding the aforementioned cooperation between the hydraulic and mechanical system, naming in the Figure 24 and the hydraulic system equations, equation (4-9) stands for the dynamical model of the steering column between the valve and the steering wheel and equation (4-10) expresses that of the valve torsional bar.

$$k_{sc}(\theta_{sw} - \theta_v) + c_{sc}(\dot{\theta}_{sw} - \dot{\theta}_v) = k_v(\theta_v - \theta_p) + c_v(\dot{\theta}_v - \dot{\theta}_p) + I_v\ddot{\theta}_v \quad \textbf{(4-9)}$$

$$k_v(\theta_v - \theta_p) + c_v(\dot{\theta}_v - \dot{\theta}_p) = I_p\ddot{\theta}_p + T_p \quad \textbf{(4-10)}$$

Also, the following relations express the dynamical model of the rack:

$$\frac{T_p}{r_p} + F_H = F_R = 2\left(K_{eq}s_R + C_{eq}\dot{s}_R\right) + m_r\ddot{s}_R \qquad \textbf{(4-11)}$$

$$\xrightarrow{s_R=\theta_p r_p} \qquad \frac{T_p}{r_p} + F_H = 2r_p\left(K_{eq}\theta_p + C_{eq}\dot{\theta}_p\right) + m_r r_p\ddot{\theta}_p \qquad \textbf{(4-12)}$$

And from equations (4-8), (4-10) and (4-12),

$$T_p = 2r_p^2\left(K_{eq}\theta_p + C_{eq}\dot{\theta}_p\right) + m_r r_p^2\ddot{\theta}_p - \frac{A}{k_2}\left(k_1\left(\theta_v - \theta_p\right) - A\rho r_p\dot{\theta}_p\right) \qquad \textbf{(4-13)}$$

Importing the above relation in equation (4-9), would results in the following state space equation for the whole system.

$$\begin{bmatrix}\dot{\boldsymbol{\theta}}_p\\ \ddot{\boldsymbol{\theta}}_p\\ \dot{\boldsymbol{\theta}}_v\\ \ddot{\boldsymbol{\theta}}_v\end{bmatrix} = \begin{bmatrix} \mathbf{0} & \mathbf{1} & \mathbf{0} & \mathbf{0} \\ -\dfrac{\boldsymbol{k_v} + \mathbf{2}\boldsymbol{K_{eq}}\boldsymbol{r_p^2} + \dfrac{\boldsymbol{k_1 A}}{\boldsymbol{k_2}}}{\boldsymbol{I_p} + \boldsymbol{m_r}\boldsymbol{r_p^2}} & -\dfrac{\boldsymbol{c_v} + \mathbf{2}\boldsymbol{C_{eq}}\boldsymbol{r_p^2} + \dfrac{\boldsymbol{A^2\rho r_p}}{\boldsymbol{k_2}}}{\boldsymbol{I_p} + \boldsymbol{m_r}\boldsymbol{r_p^2}} & \dfrac{\boldsymbol{k_v}}{\boldsymbol{I_p} + \boldsymbol{m_r}\boldsymbol{r_p^2}} & \dfrac{\boldsymbol{c_v}}{\boldsymbol{I_p} + \boldsymbol{m_r}\boldsymbol{r_p^2}} \\ \mathbf{0} & \mathbf{0} & \mathbf{0} & \mathbf{1} \\ \dfrac{\boldsymbol{k_v}}{\boldsymbol{I_v}} & \dfrac{\boldsymbol{c_v}}{\boldsymbol{I_v}} & -\dfrac{\boldsymbol{k_{sc}}}{\boldsymbol{I_v}} & -\dfrac{\boldsymbol{c_{sc}}}{\boldsymbol{I_v}} \end{bmatrix}\begin{bmatrix}\boldsymbol{\theta_p}\\ \dot{\boldsymbol{\theta}}_p\\ \boldsymbol{\theta_v}\\ \dot{\boldsymbol{\theta}}_v\end{bmatrix} + \begin{bmatrix} \mathbf{0} & \mathbf{0} \\ \mathbf{0} & \mathbf{0} \\ \mathbf{0} & \mathbf{0} \\ \dfrac{\boldsymbol{k_{sc}}}{\boldsymbol{I_v}} & \dfrac{\boldsymbol{c_{sc}}}{\boldsymbol{I_v}} \end{bmatrix}\begin{bmatrix}\boldsymbol{\theta_{sw}}\\ \dot{\boldsymbol{\theta}}_{sw}\end{bmatrix} \qquad \textbf{(4-14)}$$

4.2.2 Effects on suspension design

In Figure 25, a rack and pinion steering connection to a double wishbone suspension is shown schematically. As indicated, the tie-rods are responsible for transferring the rack's movement into the wheels, and causing them to rotate. Now, going back to the concept of the rack and pinion mechanism, it is known that when an angle is applied to pinion, the rack moves equally from each side. In other words, the displacement of the rack is the same in its connecting points to the tie-rods.

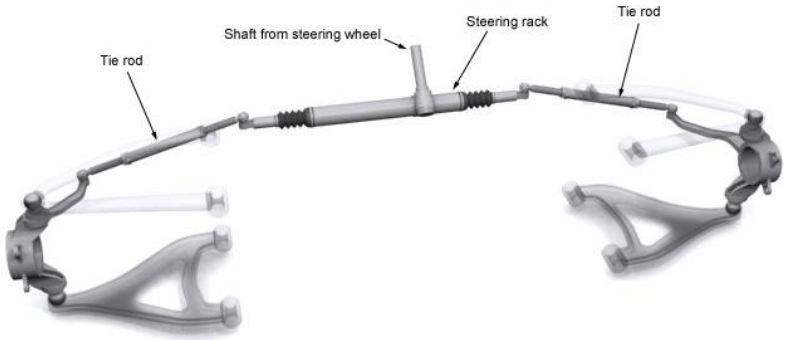

Figure 25-Schematic rack and pinion connections [54]

As discussed formerly about the steering principles, it is important that there be a specific relation between the inner and outer wheels. By what was previously mentioned, the only way of having these desired steering relations is by finding the optimal position of tie-rod connections to both the rack and the suspension. With details being described in the next chapter, the optimality of the tie-rods' connection points is dependent on both the geometry and type of suspension.

Along with all aforementioned important steering principles that should be considered in tie-rod design, it is also important to study the steering design effects on suspension characteristics. As Mentioned before, toe angle alterations by wheel travel, which is also known as steer by bump, is very important in vehicle's stability [6], and it is heavily dependent on the tie-rod's end point's position.

All in all, regarding the relations between the suspension and the steering mechanism, the rack movements along Y axis, named as ΔY_{Rack}, can be considered as one input to the suspension, and the steering angle would later play an important role in defining a proper cost function for a well-designed half-car model.

Now that the importance of the half-car analysis is explained, a mathematical definition should be provided for each suspension that explains that a wheel is inside or outside turn in relation to the rack's position.

As the steering wheel's turning direction should be the same as the vehicle's turning direction, if the installation of the rack is somehow that the tie-rod's connection point to suspension is longitudinally further than the center of the wheel, the pinion should be installed under the rack, so that when steering wheel is turning left, the pinion pushes the rack towards left side and the left wheel be inside the turn. However, if the tie-rod's connection point to suspension, X_{tr-s}, is longitudinally inner than the center of the wheel, the pinion should be installed above the rack, so that when steering wheel is turning left, the pinion pushes the rack towards right side and the tie-rod pulls the left wheel to be inside the turn[6]. Therefore,

$$\begin{cases} X_{tr-s} > X_{Wheel} & \begin{cases} \Delta Y_{Rack} > 0 & left\ wheel\ is\ inside\ the\ turn \\ \Delta Y_{Rack} < 0 & left\ wheel\ is\ outside\ the\ turn \end{cases} \\ X_{tr-s} < X_{Wheel} & \begin{cases} \Delta Y_{Rack} > 0 & left\ wheel\ is\ inside\ the\ turn \\ \Delta Y_{Rack} < 0 & left\ wheel\ is\ outside\ the\ turn \end{cases} \end{cases} \quad \textbf{(4-15)}$$

Figure 26 and Figure 27 indicate the abovementioned relations in two different steering assemblies.

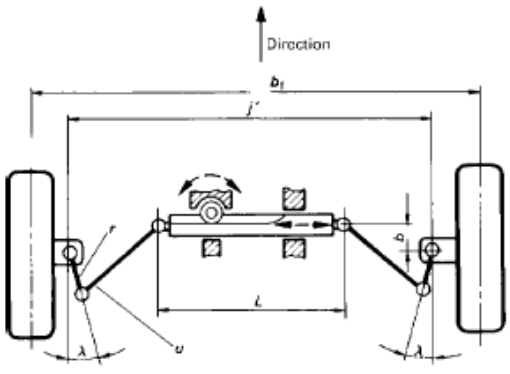

Figure 26-Rack and pinion schematic with tie-rod connection inner than wheel center [56]

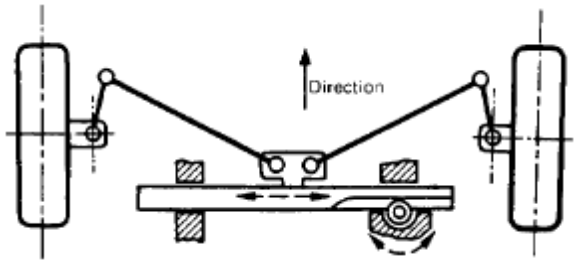

Figure 27-Rack and pinion schematic with tie-rod connection outer than wheel center [56]

4.3 Steering Kinematics

4.3.1 Ackermann Principle

The Ackermann steering principle yields the amount of steering angle on each wheel based on a kinematical analysis. To rotate without slips, all the wheels should rotate freely. As shown in Figure 28, a free rotation of each wheel means that the direction of the velocity of each wheel is along the wheel's direction. Therefore, the lines which are normal to the direction of the wheels should intersect at one point, which is also shown in Figure 29.

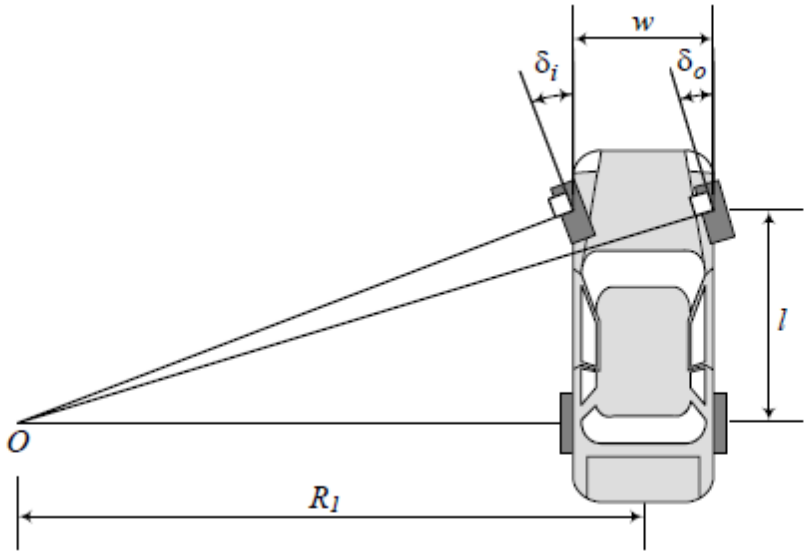

Figure 28- Ackermann geometry [1]

Now by a simple geometrical analysis, a relation between the steering angles of the inner and the outer wheel can be found.

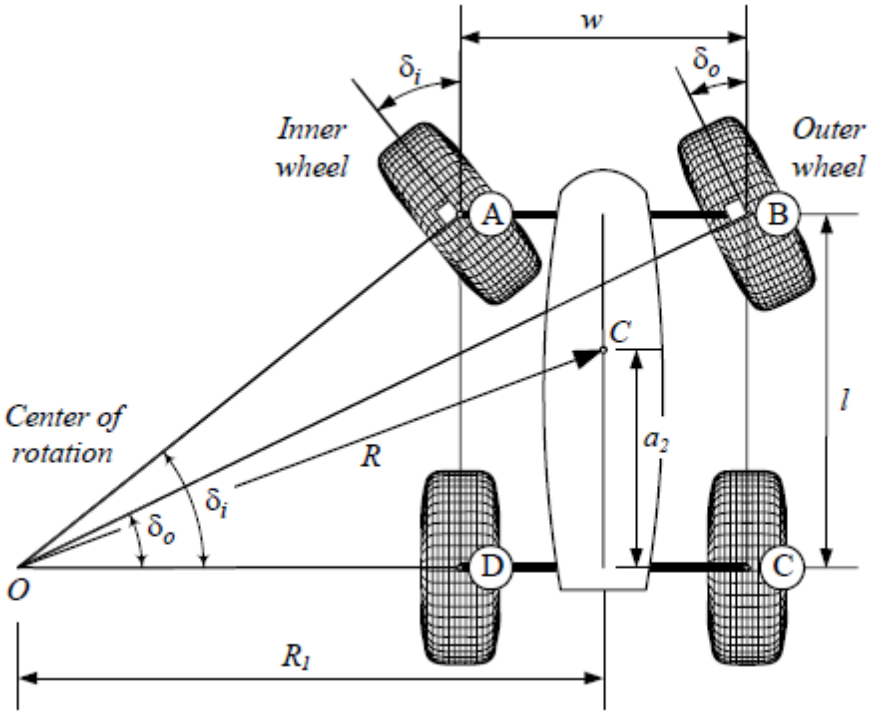

Figure 29-Ackermann geometry [1]

Considering Figure 28 and Figure 29, the steering angle of the inner wheel, named as δ_i can be found by the following geometrical relation.

$$\cot(\delta_i) = \frac{R_1 - \frac{w}{2}}{l} \qquad \textbf{(4-16)}$$

where R_1 is the turning radius of the middle of the rear axle when the vehicle's center of mass is turning around a circle with the radius of R, w is the track of the vehicle and l is the longitudinal wheel-base. These are indicated in the same pictures.

With the same approach and naming, the steering angle of the outer wheel, δ_o, is found as follows.

$$\cot(\delta_o) = \frac{R_1 + \frac{w}{2}}{l} \qquad \textbf{(4-17)}$$

Subtracting the two above equations will yield the mathematical definition of Ackermann steering principle, which is independent of the turning radius:

$$\cot(\delta_o) - \cot(\delta_i) = \frac{w}{l} \qquad \textbf{(4-18)}$$

As can be realized in the above equation, the relation between the steering angle of the inner wheel and the outer wheel is independent of the turning radius of the vehicle. However, the maximum steering angle of a vehicle, which also indicates the required movement of the links in the steering mechanism, i.e. the rack in the rack and pinion mechanism, is dependent on the minimum turning radius of a car. The turning radius of a vehicle is measured from its center of mass. Let's consider that the minimum turning radius of a vehicle is R_{Min}, and the longitudinal distance between the rear axle and the center of the mass is L_{RCG}. Regarding the geometry, one can find both $\delta_{i_{Max}}$ and $\delta_{o_{Max}}$ as follows.

$$\cot(\delta_{i_{Max}}) = \frac{\sqrt{R_{Min}^2 - L_{RCG}^2} - \frac{w}{2}}{l}$$
$$\cot(\delta_{o_{Max}}) = \frac{\sqrt{R_{Min}^2 - L_{RCG}^2} + \frac{w}{2}}{l} \qquad \textbf{(4-19)}$$

4.3.2 Anti-Ackermann

Anti–Ackermann steering is a steering concept that considers tire forces in order to have better lateral force during cornering. Tires with more loads can provide greater lateral force. This means that the tire which is outside of the turn can provide more lateral force than the inner tire, and if the inner tire wants to provide the same amount of force, it should turn more than what the Ackermann principle indicates. Therefore, it is reasonable that the tire outside the turn have a greater steering angle than the inner tire to go against the Ackermann principle. The effect of this dynamics is more pronounced at higher speeds. It should be noted that, in the case of family cars, high speed cornering is not an important issue compared its importance for racing cars. Therefore, the use of anti-Ackermann steering is not necessary in the case of family cars and the Ackermann principle should be applied.

In racing cars, although there are many arguments about anti-Ackermann pros and cons, by mirroring the vehicle's schematic from its front axle, using the naming indicated in Figure 29, the reverse Ackermann relation would be found as [30,32]:

$$\cot(\delta_i) - \cot(\delta_o) = \frac{w}{l} \tag{4-20}$$

The maximum and minimum steering angles are found with the same approach described for Ackermann principle:

$$\cot(\delta_{i_{Max}}) = \frac{\sqrt{R_{Min}^2 - L_{RCG}^2} + \frac{w}{2}}{l}$$
$$\cot(\delta_{o_{Max}}) = \frac{\sqrt{R_{Min}^2 - L_{RCG}^2} - \frac{w}{2}}{l} \tag{4-21}$$

Reverse-Ackermann is not a force analysis based approach for the best performance in cornering, and it is only a way to make the cornering performance better by a simple analysis. For optimal steering forces during cornering, force analysis shall be done. Initial toe and camber angles could be also very effective in steering efficiency [6,34,35].

Besides the reverse-Ackermann, there is the parallel steering kinematics mechanism that is used to improve vehicles performance in high-speed cornering. In parallel steering, both wheels have the same steering angle while turning and the geometry is between the pure Ackermann and the reverse-Ackermann. In Figure 30, the parallel steering geometry is compared with the anti-Ackermann and the Ackermann.

There have been many arguments about anti-Ackermann steering. Regarding load transfer, a small amount of anti-Ackermann is beneficial for racing cars and their improved performance. Also, due to the small steering angles of racing cars and the small amount of load on the inside tire, the Ackermann mechanism “cannot be right” and a small amount of static toe for better racing performance is suggested [32].

On the other hand, the Ackermann steering returned in 90’s. Having aerodynamic, downward forces is one of the reasons that the pure Ackermann steering began to be used again [35]. On the contrary, regarding scientific tire data, for optimum cornering performance, the tire with lighter load should have a higher slip angle. Therefore, the Ackermann may be useful in racing cars. However, it has been stated that the Ackermann steering may not be enough to “have a significant effect” [36].

All in all, it seems that for racing and performance cars, it is reasonable to have a small amount of anti-Ackermann steering while considering tire data in the design for optimum performance steering.

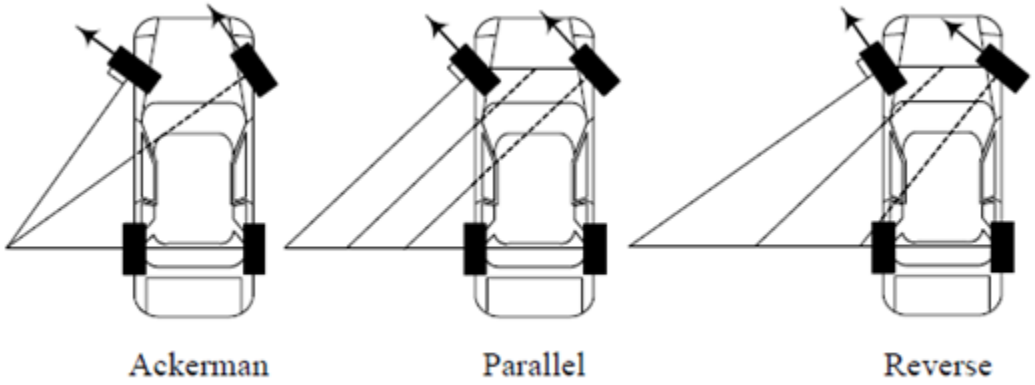

Figure 30-Different steering geometries [1]

4.3.3 Perfect steering

Regarding the mentioned concepts about the Ackermann steering principle, alongside with the effect of tire load on turning dynamics in the anti-Ackermann principle, a conclusion can be made: a vehicle has a perfect steering, if in low speeds, it uses the Ackermann steering principle, and in high speeds, it uses the anti-Ackermann principle. However, in tie rod designing, it is all about geometry, and effect of speed cannot be considered. Therefore, an engineering consideration should be applied in steering design. As mentioned, the anti-Ackermann steering is useful only when there is a huge load transfer in cornering. Considering that m is the mass, v the longitudinal speed and R the turning radius of the vehicle, the lateral force that causes lateral load transfer is found by $\frac{mv^2}{R}$. This amount cannot exceed the maximum lateral traction. Therefore, the longitudinal velocity of a car affects the load transfer more than the turning radius. Thus, in small steering angles where vehicles can have higher speeds, an anti-Ackermann steering is beneficial. In the same way, for bigger steering angles, the Ackermann principle is more beneficial.
All in all, a car which has an anti-Ackermann steering in low steering angles, i.e. 0 to 6 degrees, and Ackermann steering in high steering angles, i.e. more than 10 degrees, can provide an ideal steering efficacy.

Chapter 5
Optimization

5.1 Introduction

In everyday life, people try to choose the best of everything. They observe situations and conditions and try to do what they desire. This is a form of optimization. Every attempt at reaching an optimal solution is known as optimization. Mathematical optimization is also the same. In mathematical optimization, it is trying to find the best behavior by changing effective variables.

In mathematics, by using some methods, finding the minimum and the maximum of a function is possible. Therefore, by defining a function that includes information about the desired behaviors of a system and its variations in relation to effective variables, optimization would be possible. For instance, minimizing the error function of some data from a line leads to the fittest line, and it is known as a first degree curve fitting.

Likewise, the focus of this chapter is dedicated to defining the desired suspension in a function, so that minimizing that function provides a better design. This function is known as the cost function. Moreover, there should be some constraints to prevent impossible geometry settings for a suspension. These constraints may also include static requirements of the suspension, such as a small negative caster angle. In this thesis, the cost function is based on L^2 norm with different weights on different desired characteristics. The detailed definition of cost function is provided in the following sections as well as the physical constraints of both the MacPherson and the double-wishbone suspension types.

5.2 Cost Function Definition

As previously shown in the "Suspension" chapter, all dynamically important characteristics of suspension are found by solving the mathematical model of suspension systems, and equations (3-29) to (3-31) indicated the most important characteristics of suspension.

By finding these characteristics and using the L^2_{norm} error definition, a general cost function can be defined. At each point of wheel travel, an error vector exists ($\mathrm{E}(\Delta z_{wheel})$), whose components indicate the difference between desired value and real value at maximum, zero, and minimum steering angles respectively. If i points at a specific characteristic, and i_d be the desired value for that characteristic, at each steering angle we have:

$$\epsilon_i(\Delta z_{wheel}) = (i(\Delta z_{wheel}) - i_d(\Delta z_{wheel})) \quad \textbf{(5-1)}$$

Now, regarding (5-1), each E(Δz_{wheel}) is described as:

$$\begin{aligned}\mathbf{E}(\boldsymbol{\Delta z_{wheel}})_k = \boldsymbol{w_1}\left(\boldsymbol{\epsilon_{Toe}}(\Delta z_{wheel})\right)_k + \boldsymbol{w_2}\left(\boldsymbol{\epsilon_{Camber}}(\Delta z_{wheel})\right)_k + \boldsymbol{w_3}\left(\boldsymbol{\epsilon_{Track}}(\Delta z_{wheel})\right)_k \\ + \boldsymbol{w_4}\left(\boldsymbol{\epsilon_{Caster}}(\Delta z_{wheel})\right)_k + \boldsymbol{w_5}\left(\boldsymbol{\epsilon_{Kingpin}}(\Delta z_{wheel})\right)_k\end{aligned} \quad \textbf{(5-2)}$$

Now, let:

$$\boldsymbol{j}(\Delta z_{wheel}) = \mathbf{E}(\Delta z_{wheel})_k^{\boldsymbol{T}}.\mathbf{E}(\Delta z_{wheel})_k \quad \textbf{(5-3)}$$

Thus, a cost function ($J_{wheelTravel}$) can be defined based on equation (5-3) as follows:

$$\begin{aligned}\boldsymbol{J_{Wheel\,Travel}} = \boldsymbol{W_{Low}}\left(\int_{-80}^{-30}\boldsymbol{j}(\Delta z_{wheel}).\boldsymbol{d\Delta z_{wheel}}\right) + \boldsymbol{W_{Mid}}\left(\int_{-30}^{+30}\boldsymbol{j}(\Delta z_{wheel}).\boldsymbol{d\Delta z_{wheel}}\right) \\ + \boldsymbol{W_{High}}\left(\int_{+30}^{+80}\boldsymbol{j}(\Delta z_{wheel}).\boldsymbol{d\Delta z_{wheel}}\right)\end{aligned} \quad \textbf{(5-4)}$$

In the above equations, d subscript stands for the desired value of the characteristic and w_i is the weight for each characteristic, k stands for the steering angle that values are calculated for, W stands for the weight which specifies the importance of design accuracy regarding the position of the center of the wheel on the Z Axis and w refers to the weight that specifies the importance of each characteristic.
On the other hand, as mentioned in the "Steering" chapter in detail, the steering principle design should be also considered in the cost function. Therefore, an error function, named $\epsilon_{Steering}$, is described in equation (5-5) to show the difference between the desired steering angle and the real steering angle.:

$$\epsilon_{Steering}(\Delta y_{Rack}) = \left(\Delta\delta_{steering-real}(\Delta y_{Rack}) - \Delta\delta_{steering-desired}(\Delta y_{Rack})\right) \quad \textbf{(5-5)}$$

Using this description, with the same approach used for function ($J_{wheelTravel}$), the cost function of steering is found by the relations showed in equations (5-6) and (5-7).

$$\boldsymbol{j}(\Delta y_{Rack}) = \epsilon^2{}_{Steering}(\Delta y_{Rack}) \quad \textbf{(5-6)}$$

$$\boldsymbol{J_{Steering}} = \boldsymbol{W_{Steering}}\left(\int_{\boldsymbol{Min}}^{\boldsymbol{Max}}\boldsymbol{j}(\Delta y_{Rack}).\boldsymbol{d\Delta y_{Rack}}\right) \quad \textbf{(5-7)}$$

Finally, the final cost function would be:

$$J = J_{Wheel\,Travel} + J_{Steering} \tag{5-8}$$

5.3 Constraints

5.3.1 MacPherson Suspension

A schematic view of a MacPherson suspension was provided in Figure 11. Considering the same names, equalities and inequalities can be shown simply.

Geometry wise, for a MacPherson suspension at the left side of the vehicle following the general constraints must be active.

1) Points A, B and C should be more inside than the wheel's mounting point.

$$\begin{gathered} y_A < y_P \\ y_B < y_P \\ y_{C_0} < y_C < y_P \end{gathered} \tag{5-9}$$

2) The control arm's mounting points to the chassis must be more inside than point A.

$$\begin{gathered} y_D < y_A \\ y_E < y_A \end{gathered} \tag{5-10}$$

3) Point B_0 is the connecting point of tie-rod to steering mechanism; therefore, it should be more inside than B, which is the end of tie-rod.

$$y_{B_0} < y_B \tag{5-11}$$

4) The following relations must be satisfied regarding the points' heights.

$$\begin{gathered} z_A < z_P < z_C < z_{C_0} \\ z_A < z_B < z_B \end{gathered} \tag{5-12}$$

5) As steering direction should not change, the following constraint must be considered between tie-rod ends and wheel's center point.

$$x_{B_0} < x_B < x_P \tag{5-13}$$

6) Steering is normally designed with considerations that make length of tie-rod and point B_0 fixed, as is mentioned mathematically below.

$$\left|\overrightarrow{B_0B}\right|_{Designed} = \left|\overrightarrow{B_0B}\right|_{Initial}$$
$$B_{0_{Designed}} = B_{0_{Initial}} \tag{5-14}$$

7) Point P_1, the initial position of point P cannot be designed, as is related to prior levels of vehicle design.

$$P_{1_{Designed}} = P_{1_{Initial}} \tag{5-15}$$

5.3.2 Double-Wishbone Suspension

Below, a schematic view of a double-wishbone suspension, whose points are named, is provided.

Considering the names for writing equalities and inequalities, one can simply define basic constraints as well.

Like the MacPherson suspension, for a double-wishbone suspension at left side of vehicle there are at least the following general constraints regarding to geometry.

1) All the spindle hard-points must be more inside than the center of the wheel, formerly expressed in Equation (5-10).
2) The lower-wishbone's mounting points to the chassis must be more inside than the ball joint of wishbone, Equation (5-11).
3) B_0 is the connection of tie-rod and steering mechanism; therefore, it should be more inside than B, which is the end of tie-rod and is represented in Equation (5-12)
4) The following relations must be satisfied regarding the points' heights.

$$z_A < z_P < z_C$$
$$z_A < z_B < z_C \tag{5-16}$$

5) Similar to equation (5-14), the steering direction should not change, and the following constraint must be considered between tie-rod ends and wheel's center point.
6) The "fire-wall" is fixed, as is described in equation (5-15)

All other constraints are limits that can be variable regarding different design circumstances; therefore, they can be written generally as follows.

$$(Initial\ Point)_i - a_i \leq (Design\ Point)_i \leq (Initial\ Point)_i + b_i \qquad \textbf{(5-17)}$$

Where a_i and b_i indicate the range that design flexibility of each point is possible regarding engineering restricted circumstances. For example, a vehicle that has been previously but requires a more optimal suspension behavior may not allow designer to change mounting points at all. Meaning that the inequality provided by (5-17) yields fixed point equality at mounting points, as a_i and b_i become zero in this special case.

For scrub radius, kingpin inclination angle and caster angle a desired initial guess is necessary, along with calculations that indicate the desired boundaries of them relative to the affecting points. Then, the constraints can be applied using those boundaries in equation (5-17).

Chapter 6
Case Study

In this chapter, an analysis has been provided on the front suspension of the Peugeot 405, produced by Iran Khodro Company, to study the characteristics of this family car and compare them with desired behaviors of family cars. Then, an attempt has been made to verify the optimization concepts of this thesis by comparing results with the same vehicle. Later, the mentioned suspension is used as an initial guess, and it is optimized to reach sports car characteristics. The last case study is applying the knowledge of suspension kinematics to design a suspension for a SUV. For this purpose, the wheel dimensions of a 2012 Land Cruiser V8 is considered.

6.1 Family car

In this part, a MacPherson suspension is studied. The suspension dimensions belong to a family car which has been produced from 1987 to 1997, in Europe, and assembled from 1987 up to now, in Iran and Egypt, by Peugeot and Iran Khodro Companies respectively. Studying such a successful car can lead to a better understanding of family car requirements. It also can help to verify optimization concepts mentioned in previous chapters. In
Table 1- Peugeot 405 suspension dimensions, the dimensions of the suspension hard points are shown.

6.1.1 Analysis

The analysis is divided to three sections:

- Studying the effects of wheel travel on suspension characteristics while no steering is applied.
- Considering no vertical wheel travel and studying the steering kinematics and effects on desired behaviors.
- Analyzing reactions of the system while both steering and vertical wheel travel are applied.

Table 1- Peugeot 405 suspension dimensions

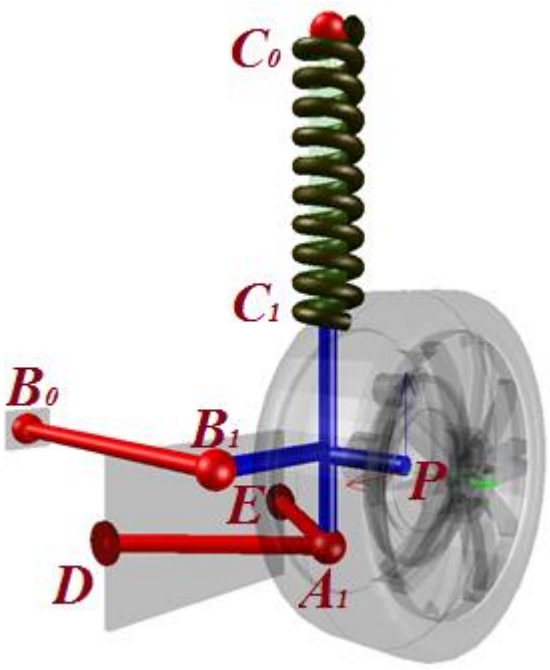

Position Name	Optimized Position
x_{A_1}	503.46
y_{A_1}	687.25
z_{A_1}	191.5
x_{B_1}	639.178
y_{B_1}	664.471
z_{B_1}	292.165
x_{C_0}	534.42
y_{C_0}	567.875
z_{C_0}	868.4
x_{C_1}	525.478
y_{C_1}	583.66
z_{C_1}	403.968
x_D	789.02
y_D	379.5
z_D	259.37
x_E	501.17
y_E	379
z_E	243.67
x_{B_0}	670.85
y_{B_0}	312.5
z_{B_0}	341
x_P	509.23
y_P	748.94
z_P	279.66
R_{Wheel}	300

6.1.1.1 Wheel travel effects with no steering

In this section, the focus of study is on the effects of vertical wheel travel. The amount of wheel travel is considered to be as same as the standard bump [17]. Wheel travel is positive when there is a reduction in the distance between wheel and body, known as jounce.

Toe angle changes, track alterations and camber angle variations are the most important characteristics being affected by wheel travel. As mentioned in previous chapters, toe angle changes must be as minimal as possible. High amounts of toe angle variation can cause unwanted steering while subsequently endangering passengers. Therefore, a good family car should avoid huge variations of toe angles. Figure 31 shows the toe changes while the wheel travels from -80 mm to 80 mm in the standard Z direction.

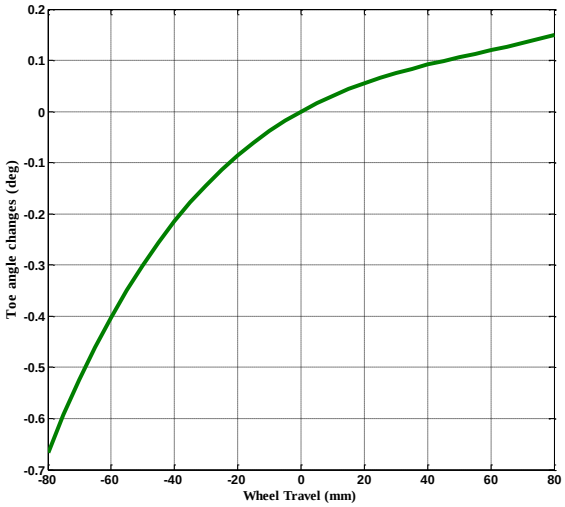

Figure 31- Toe angle changes vs. wheel travel at zero steering input

As it can be seen in the above figure, toe change is less than 1 degree at it maximum, which indicates a good designed suspension. However, it is not the only issue to be considered. A family car must reduce maintenance expenses. Therefore, track alterations, which are the most important behavior of a suspension regarding tire wear and erosion, should be very low during vertical displacement. Figure 32 demonstrates track variations by wheel travel. As shown, the maximum alteration is about 25 mm, a very low alteration in track which happens at jouncing. At jouncing, there is less load on the tire subsequently reducing tire erosion.

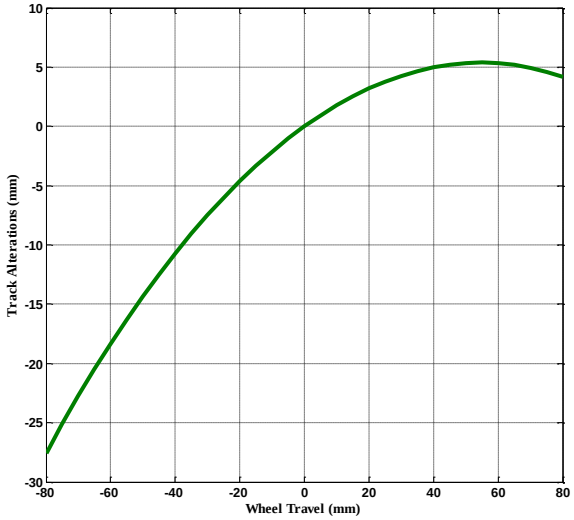

Figure 32-Track alterations vs. wheel travel with no steering input

As mentioned in the "Suspension" chapter, camber variations should also be small. The camber angle can provide lateral forces and cause unwanted steering. However, the amount of force it can provide is negligible when it is lower than 5 degrees. Figure 33 illustrates the camber changes of the Peugeot 405 during vertical movements of the wheel. As can be seen, the maximum error happens during rebound when the load is lower than usual, and this situation minimizes the lateral force caused by the camber angle. Though, even the maximum amount of camber in this car is not enough to endanger the safety of passengers.

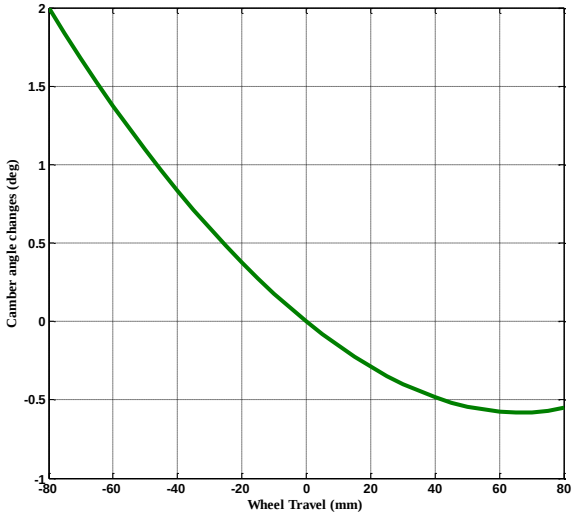

Figure 33-Camber angle changes vs. wheel travel with no steering input

6.1.1.2 Steering effects with no wheel travel

As explained formerly, family cars should minimize maintenance expenses. Another issue that causes tire erosion is a steering that does not provide the Ackermann geometry. Therefore, in a family car, the steering mechanism should satisfy the Ackermann conditions. Figure 34 illustrates the differences between pro-Ackermann steering and the studied car's steering.

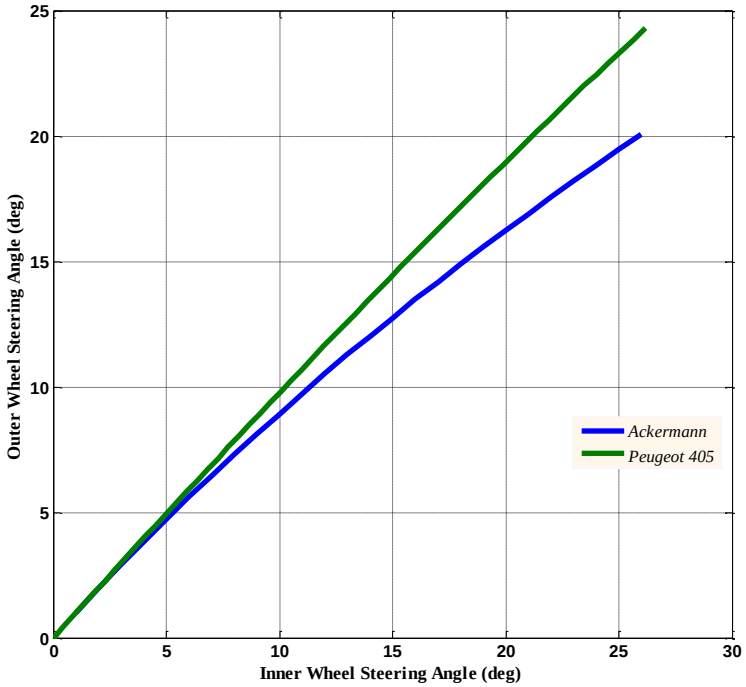

Figure 34- Steering characteristic of the studied car vs. Ackermann for $w = 1.7145\ m$ and $L = 2.5\ m$.

Although the vehicle does not show a pro-Ackermann relation between the wheels, it tends toward having a small amount of anti-Ackermann, which is a good idea for having a better steering while cornering fast. Moreover, as will be discussed in the next case study, this steering has the minimum error from a pro-Ackermann after considering all important behaviors in the cost function.

Another cause of tire erosion is track alteration while steering is applied. It is necessary to minimize track variations while steering because it not only affects tire erosion, but it also has a slight impact on changing the lateral force. Figure 35 clearly illustrates good track alterations for a family car. Furthermore, it shows the amount of track variations in both inner and outer wheels during a turn. The amount of change is impressively low for the outer wheel, which bears more load in cornering, so fewer track alterations are necessary.

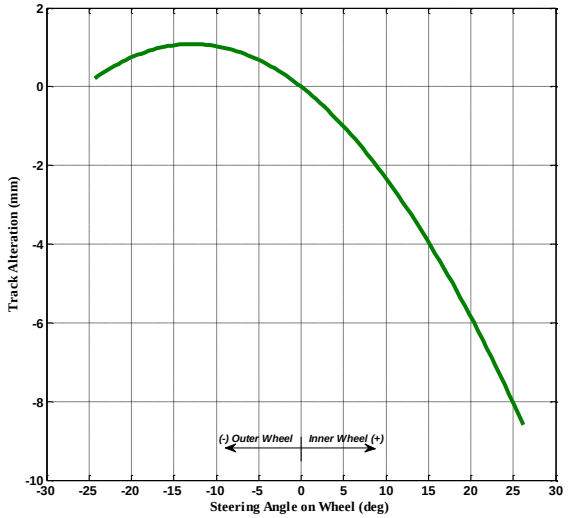

Figure 35- Track alterations vs. steering angle

6.1.1.3 Wheel travel effects on steering

This part of the analysis studies toe angle changes by vertical wheel travel when steering is also applied to the wheels. Losing the control of the steering wheel in cornering can be extremely dangerous. If a vehicle travels through bumps while turning, control loss could happen. Also, when the amount of roll is high, the wheel travel caused by this roll can further amplify the problem. This phenomenon is known as "steering error". To minimize this danger, the suspension should prevent notable amounts of toe angle changes in these situations. The graph below shows the small steering error in maximum steering versus wheel travel for both inner and outer wheels.

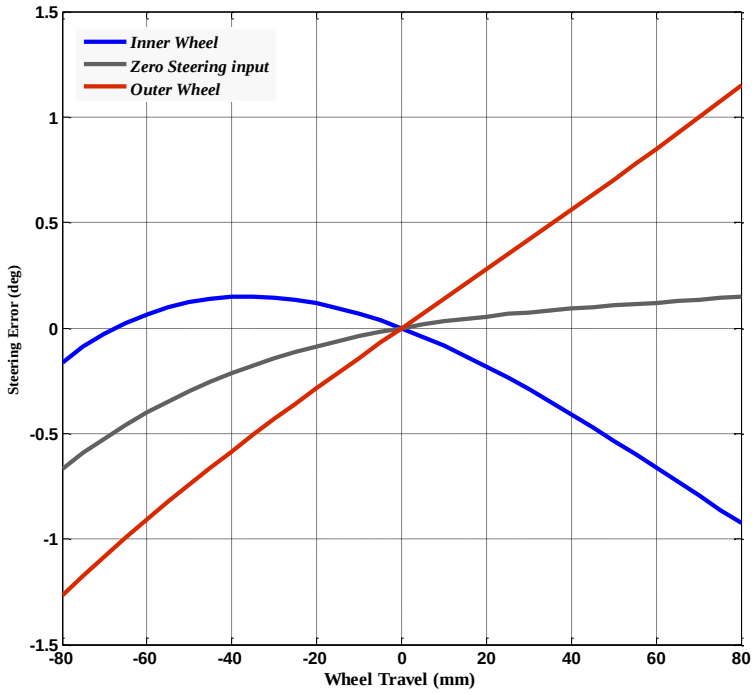

Figure 36- Steering error in maximum steering vs. wheel travel

Altogether, the entire suspension and steering characteristics of the Peugeot 405 explains the reasons of its success and popularity. This suspension meets all the requirements of a family car's suspension. Therefore, it can be used to examine the optimization methods that are discussed in this thesis. In the next part, an attempt has been made to show the accuracy of optimization concepts of this study.

6.1.2 Optimization

Now that a family car has been studied, by using the cost function provided in the "Optimization" chapter, one should examine the results. For verification, two steps are required. First, the initial geometry is fed into the function in MATLAB, and the fmincon function is used to find the local optimum geometry for the suspension and compare these changes. Then, the geometry of some crucial hard points are changed in an attempt to find the optimal geometry with the same cost function and constraints. If both steps yield the same result as the family car, or the results are very similar, the optimization has passed the exam and can be used for further designs.

For tuning the weights of the cost function, it is important to know what type of vehicle is under study. Family cars should show a very small amount of toe angle and track variations during wheel travel. Moreover, the track alterations by steering should be small. Toe-by-wheel travel during steering should be minimized, and the steering goal is a pro-Ackermann steering geometry. On the other hand, camber angle changes should be minimized and should not exceed 5 degrees. The weight of each matter as considered is shown in Table 2:

Table 2- Characteristics weights

Characteristic	Weight
Camber	*1*
Toe	*10*
Track	*5*

The weights are the same for both steering and wheel travel. Also, other weights are applied depending on the position of the wheel. Positions near the working point are considered to be more important in relation to the issues discussed about fast turning and wheel travelling. These weights are indicated in the following table.

Table 3- Weights of inputs intervals

		Steering Angle (deg)		
		$\delta_{min} \rightarrow \frac{1}{3}\delta_{min}$	$\frac{1}{3}\delta_{min} \rightarrow \frac{1}{3}\delta_{max}$	$\frac{1}{3}\delta_{max} \rightarrow \delta_{max}$
Wheel Travel (mm)	$40 \rightarrow 80$	1.5	4.5	2.5
	$-40 \rightarrow 40$	3	9	5
	$-80 \rightarrow -40$	1	3	1.5

The cost function of the steering principle is also added to suspension's cost function with a weight of 90, which is equal to the weight of toe changes near the working point of the wheel.

For both first and second steps, the end points of the tie-rod and the end point of the control arm are chosen as free to change ± 10 cm, shown in Figure 37. The scrub radius, inclination angle, and caster angle are statically constrained to be positive and in a practical range.

The results for the first step were proved to be the local minimum, resulting in exit flag number 4 of fmincon function.

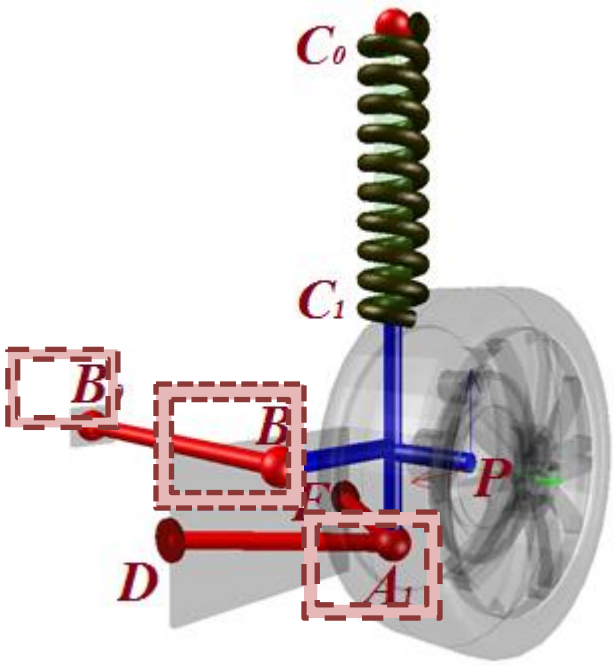

Figure 37-Free to change hard points

Now, the second step of verification should be taken. The control arm's ball joint position is known to be a critical point. The inclination angle, scrub radius, caster angle and roll center are the most important static characteristics that depend on the position of this point. It also shows its importance in track and camber control. This point has been taken to its limit and the tie-rod's ends are free to move about 10 cm from their initial point in any direction with no constraints on tie-rod length. It is assumed that with a good cost function, trying to reach an Ackermann steering should be enough.

In this case, the result was slightly different and a total change of 4 mm is observed, which belongs to tie-rod only. These variations are negligible and can be due to the importance of toe minimization in this study, as is observed in Figure 38. Table 4 indicates the initial and the optimized dimensions. Optimized geometry is very similar to the Peugeot 405.

Table 4- Changed vs. optimized dimensions

Position Name	Optimized Position	Initial Position
x_{A_1}	503.4	480
y_{A_1}	687.2	600
z_{A_1}	191.5	191.5
x_{B_1}	639.2957	639.178
y_{B_1}	664.2733	664.471
z_{B_1}	290.6329	292.165
x_{C_0}	534.42	534.42
y_{C_0}	567.875	567.875
z_{C_0}	868.4	868.4
x_{C_1}	525.478	525.478
y_{C_1}	583.66	583.66
z_{C_1}	403.968	403.968
x_D	789.02	789.02
y_D	379.5	379.5
z_D	259.37	259.37
x_E	501.17	501.17
y_E	379	379
z_E	243.67	243.67
x_{B_0}	670.7743	670.85
y_{B_0}	312.7559	312.5
z_{B_0}	342.7497	341
x_P	509.23	509.23
y_P	748.94	748.94
z_P	279.66	279.66
R_{Wheel}	300	300

Despite toe angle changes and track alterations, no other characteristic's changes are visual, i.e. as shown by Figure 39 about camber changes. The changes of toe and track are also slightly different from the basic family car. Figure 38 and Figure 39 demonstrate the slight differences caused by these negligible changes.

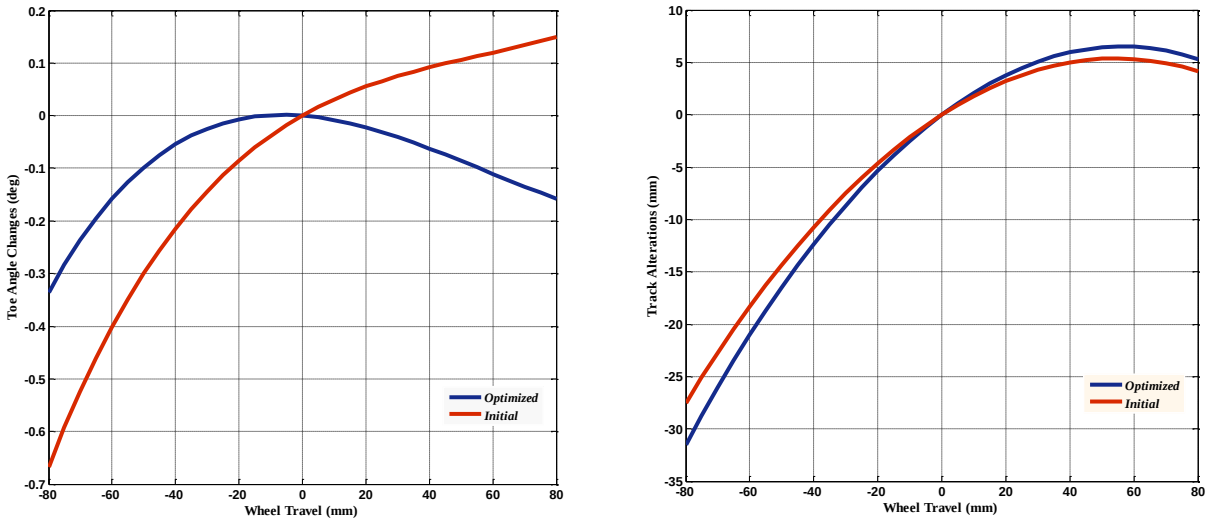

Figure 38- Toe angle changes (left) and Track alterations (right) by wheel travel; Comparing optimized suspension and Peugeot 405

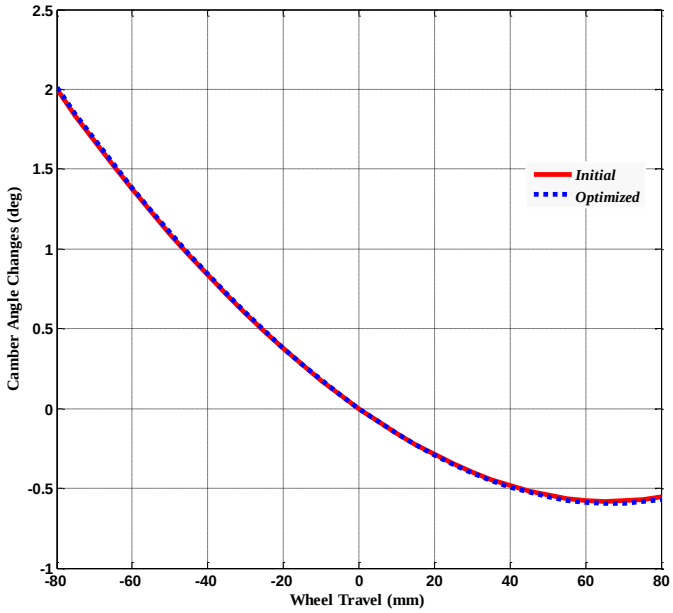

Figure 39- Camber angle changes by wheel travel; Comparing optimized suspension and Peugeot 405

6.2 Sports car

In previous sections, the vehicle optimization concepts that were discussed have been verified. Therefore, they can be used in designing new suspensions or optimizing the performance of an existing suspension. In this section, the objective is to reach sports car behaviors by optimizing a family car. Considering the sports car requirements, an attempt has been made to optimize the suspension of the Peugeot 405, which was discussed and shown to have a great suspension for a family car.

A sports car needs high performance, but tire wear is not an important issue in their design. Therefore, minimizing toe variations should be the priority along with an anti-Ackermann steering principle. Track variations by steering in small steering angles should be very small as well. More negative camber in bump and more positive camber in bump can be desirable due to the effects of roll on wheel travel.

For this optimization, the weights of cost function are shown from Table 5 to Table 7.

Table 5- Characteristics weights

Characteristic	Weight
Camber	*2*
Toe	*15*
Track	*5*

The weights are the same for both steering and wheel travel.

Table 6- Weights of inputs intervals for Toe

		Steering Angle (deg)		
		$\delta_{min} \rightarrow \frac{1}{3}\delta_{min}$	$\frac{1}{3}\delta_{min} \rightarrow \frac{1}{3}\delta_{max}$	$\frac{1}{3}\delta_{max} \rightarrow \delta_{max}$
Wheel Travel (mm)	$40 \rightarrow 80$	2	6	4
	$-40 \rightarrow 40$	3	9	7.5
	$-80 \rightarrow -40$	1	3	1.5

Table 7- Weights of inputs intervals for Track and Camber

		Steering Angle (deg)		
		$\delta_{min} \rightarrow \frac{1}{3}\delta_{min}$	$\frac{1}{3}\delta_{min} \rightarrow \frac{1}{3}\delta_{max}$	$\frac{1}{3}\delta_{max} \rightarrow \delta_{max}$
Wheel Travel (mm)	$40 \rightarrow 80$	1	6	1
	$-40 \rightarrow 40$	2	9	2
	$-80 \rightarrow -40$	1	3	1

The cost function of the reverse-Ackermann steering is also added to suspension's cost function with a weight of 135, which is equal to the weight of toe changes near the working point of the wheel.
In regards of the points that should be changed, the end of the control arm and two ends of the tie-rod are a must. Also, one can reach better characteristics by changing the connection between the strut and the spindle. These points are shown in the following schematic.

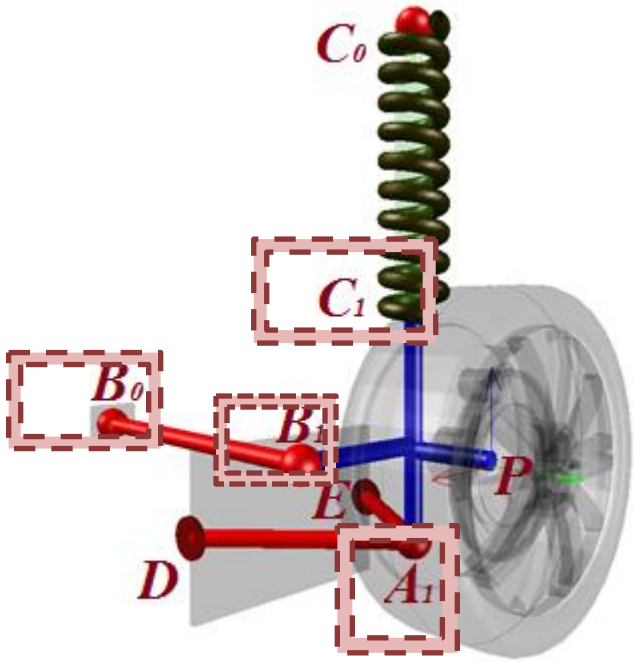

Figure 40- Points free to change for optimization

Now, by feeding the Peugeot 405's dimensions into the optimizer, using the former static constraints, and allowing each hard point a ± 10 cm of movement, the optimized positions can be found. Table 8 demonstrates the comparison between the two suspensions.

Table 8- Optimized dimensions and initial family car

Position Name	Optimized Position (Sport Car)	Initial Position (Peugeot 405)
x_{A_1}	511.023	503.46
y_{A_1}	637.25	687.25
z_{A_1}	141.5	191.5
x_{B_1}	700	639.178
y_{B_1}	676.7976	664.471
z_{B_1}	288.891	292.165
x_{C_0}	534.42	534.42
y_{C_0}	567.875	567.875
z_{C_0}	868.4	868.4
x_{C_1}	545.478	525.478
y_{C_1}	563.66	583.66
z_{C_1}	403.7645	403.968
x_D	789.02	789.02
y_D	379.5	379.5
z_D	259.37	259.37
x_E	501.17	501.17
y_E	379	379
z_E	243.67	243.67
x_{B_0}	670.85	670.85
y_{B_0}	362.5	312.5
z_{B_0}	391	341
x_P	509.23	509.23
y_P	748.94	748.94
z_P	279.66	279.66
R_{Wheel}	300.0	300

With these changes in the suspension, results seem to show an acceptable high-performance sports car. In the figures provided, the new characteristics are shown along with the initials for a better comparison. Figure 41 represents the camber changes vs. wheel travel. As visible, the optimized car shows a more negative camber in positive wheel travel, and a more positive camber angle in negative wheel travel. This speaks toward good camber behavior in regards to cornering.

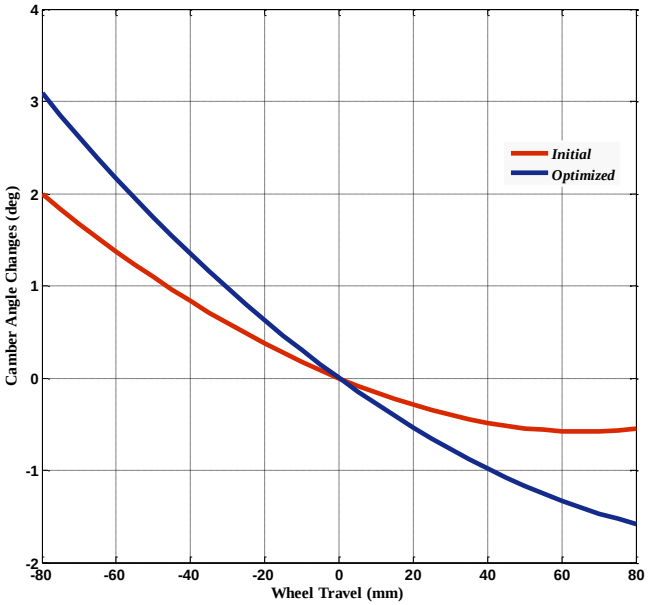

Figure 41- Camber by Bump at Zero Steering

The other important issue in camber change is that it should not be more than 5 degrees. The reason is because of straight driving situations. Bump travelling should not cause a large enough camber angle for notable lateral force to be pushed onto the vehicle in high speeds. As it also should not cause over steer, only a slight camber is desirable during fast cornering.

The next two figures show the effect of optimization on toe angle changes with wheel travelling, in both no steering input and maximum steering. Toe variations have decreased; in fact, the most amount of this decrease belongs to the negative wheel travel. In positive wheel travelling, it may seem to be worse, however, this is due to the attention of the cost function on minimizing the error while steering is applied as well. As can be seen in Figure 43, wheel travel does not affect the outer wheel's steering error and it is very desirable.

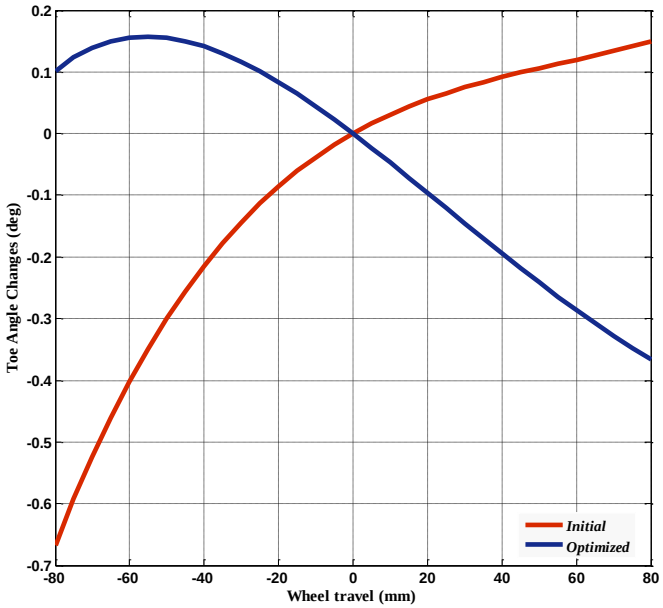

Figure 42-Toe Changes vs Bump at zero Steering

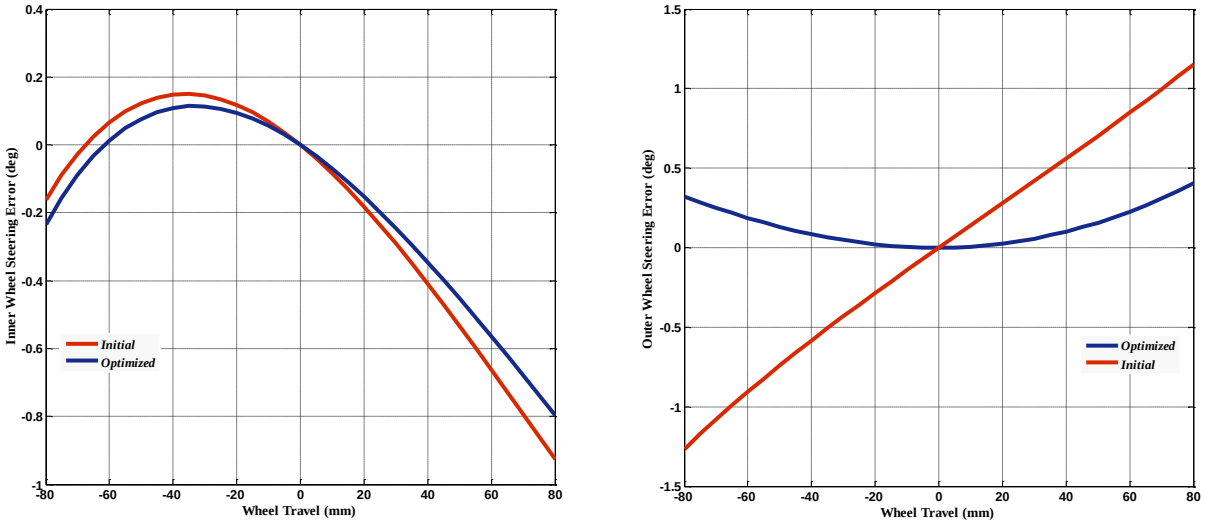

Figure 43-Toe Changes vs Bump at Maximum Steering for outer wheel, left, and inner wheel, right

According to the desired track alterations in sports cars, an attempt was made to reduce the amount of track variations by steering and focusing on small steering angles. This is perfectly shown in Figure 44.

Steering angle being between ± 6 degrees, which is considered as a small angle, these track variations are smaller than the family car.

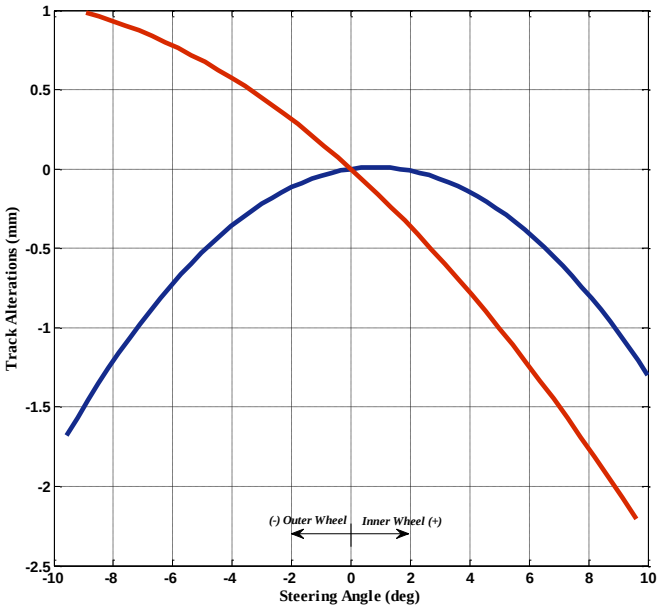

Figure 44-Track Alterations vs steering Zero Bump

Although results are better while steering, Figure 45 shows that there would be a huge track change in the sports car during normal wheel travel. This can cause a very high tire wear and should be entirely avoided in family cars.

By the following figure, it will be observed that in positive wheel travel, which can be caused by high roll angles due to fast cornering, track variations are not desired. This happens as a tradeoff between a perfect reverse-Ackermann steering and track variations, as is illustrated in Figure 46.

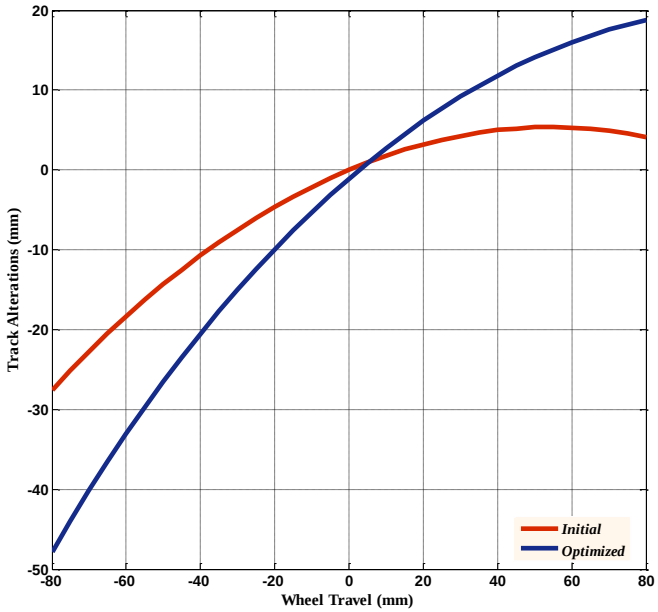

Figure 45-Track Alterations vs Bump at zero steering

The last figure of this section belongs to the steering behaviors of the optimized car. There are four curves shown in Figure 46. The first curve, in green, presents the reverse-Ackermann geometry. The second one, in blue, represents the steering behavior of the optimized car. The third, in red, shows the behavior of the family car, and the last curve illustrates the pro-Ackermann geometry. As it can be understood by these curves, the optimized suspension has only a slight difference with the reverse-Ackermann geometry. This can immensely improve the handling performance of the sports car due to rationales mentioned in the chapter titled, “Steering”.

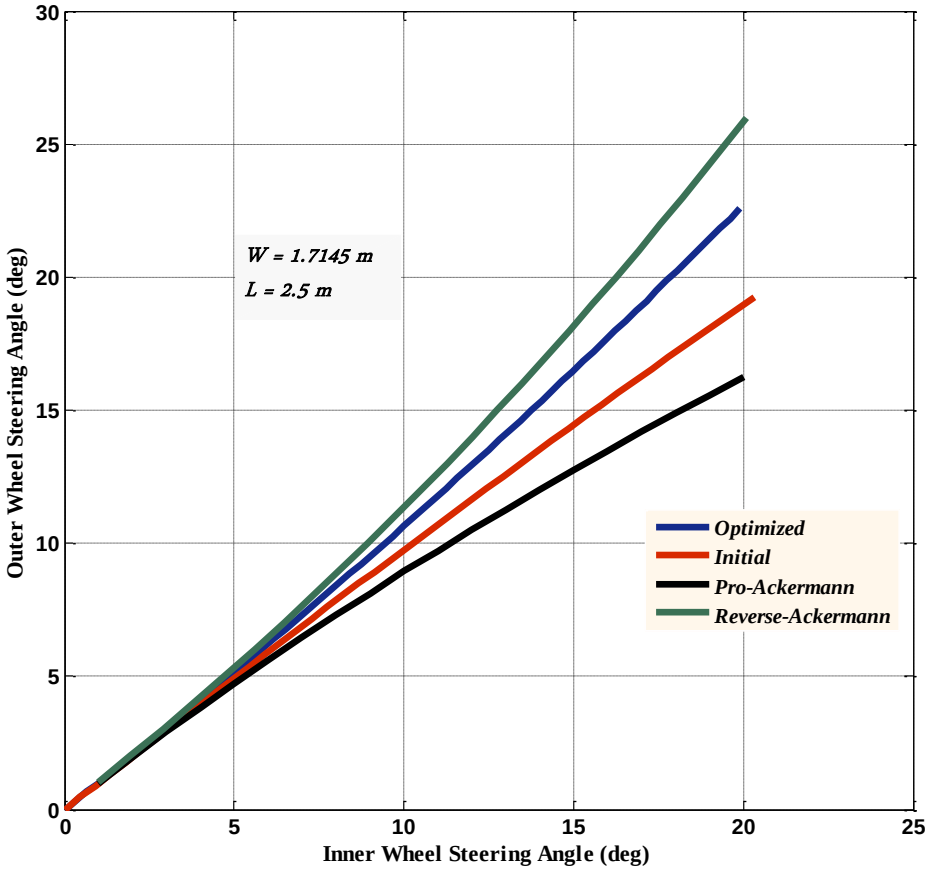

Figure 46-Steering characteristic of the family car and the optimized car

6.3 SUV

In this section, an attempt has been made to design a good suspension for a SUV, whose wheels, wheel base and track are considered to be the same as a Land Cruiser V8 2012.

6.3.1 Analysis

The initial geometry is defined by rules that have been mentioned in suspension design books [6]. After finding the initial geometry, one should analyze the characteristics to study the behavior of the designed system. In Table 9, the geometry of the initial suspension is provided based on the naming provided in Figure 13.

Table 9- Initial SUV suspension geometry

Position Name	Initial Position (mm)
x_A	9.8
y_A	-10
z_A	-187
x_B	150
y_B	-48.39
z_B	11.31
x_{C_0}	-11
y_{C_0}	-356.77
z_{C_0}	160
x_C	-11
y_C	-65.77
z_C	210
x_D	-250
y_D	-410
z_D	-187
x_E	150
y_E	-410
z_E	-187
x_{B_0}	190
y_{B_0}	-451.56
z_{B_0}	4.11
x_P	0
y_P	0
z_P	0
R_{Wheel}	400

By this geometry, Figure 47 and Figure 49 represent the behaviors of the initial guess. The first figure shows reasonable camber changes by wheel travel.

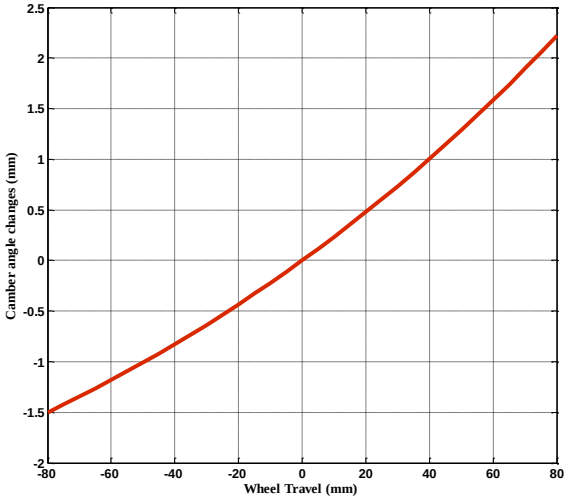

Figure 47- Initial Camber Angle variations by wheel travel

However, Figure 48 also shows a considerable amount of toe angle changes by wheel travel which is not desirable, especially that there are 3 degrees of change at jouncing. Therefore, more focus should be dedicated to toe variations during the optimization process. On the other hands, the track alterations are reasonable by both steering and wheel travel. This is clearly indicated in Figure 49.

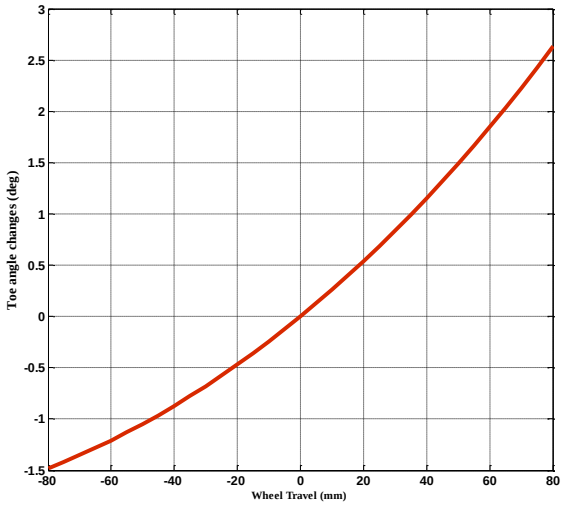

Figure 48-Initial guess Toe angle changes by wheel travel

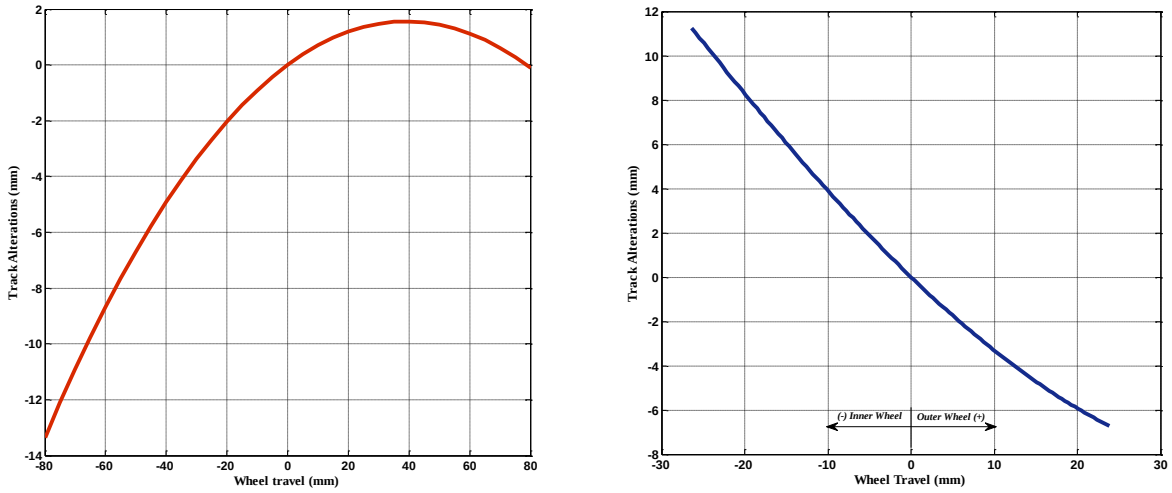

Figure 49- Initial guess Track Alterations by Wheel travel, on the left, and Steering on the right

6.3.2 Optimization

In this part, in relation to the analysis section, the main focus should be on toe angle variations. The second important criteria would be track alterations by steering, and the desired steering being set to parallel steering. The reason for these criteria is the height of a SUV. As the center of mass is considerably above the ground in SUVs, while cornering, there would be more load transfer and subsequently, the Ackermann principle may not fully satisfy the desired lateral force. On the other hand, a SUV is not used as a competition car and will not steer harshly during a turn. Therefore, the reverse-Ackermann is too much for the steering. Consequently, a parallel steering can satisfy this situation better.

In this case study, most of the hard points can be changed ± 10 cm and the cost function weights are the same as Table 2 and Table 3.
Table 10 indicates the changed positions.

Table 10-Optimized geometry vs. Initial

Position Name	Optimized Position	Initial Position
x_A	4.80000000000000	9.8
y_A	-60	-10
z_A	-197.153720290092	-187

x_B	**185**	**150**
y_B	**-17.4677248310190**	**-48.39**
z_B	**61.3100000000000**	**11.31**
x_{C_0}	**-11**	**-11**
y_{C_0}	**-381.770000000000**	**-356.77**
z_{C_0}	**185**	**160**
x_C	**-6**	**-11**
y_C	**-80.7700000000000**	**-65.77**
z_C	**190**	**210**
x_D	**-250**	**-250**
y_D	**-460**	**-410**
z_D	**-177**	**-187**
x_E	**150**	**150**
y_E	**-410**	**-410**
z_E	**-187**	**-187**
x_{B_0}	**240**	**190**
y_{B_0}	**-376.560000000000**	**-451.56**
z_{B_0}	**60.6747640313509**	**4.11**
x_P	**0**	**0**
y_P	**0**	**0**
z_P	**0**	**0**
$\boldsymbol{R_{Wheel}}$	**400**	**400**

The above geometry yields improvements in toe, track and camber alterations as indicated in Figure 50, Figure 51 and Figure 52 respectively. A great improvement is achieved for toe angle variations. Also, track behavior by steering is improved and camber angle variations are even less than before.

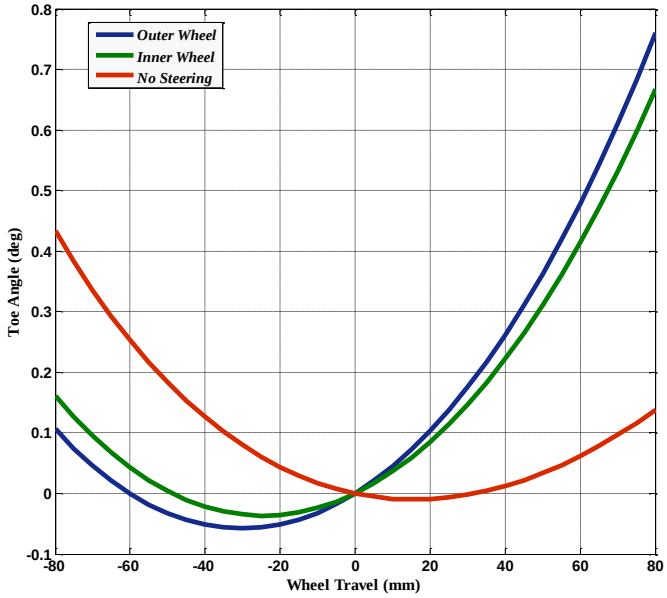

Figure 50- Toe angle Changes by Wheel Travel in maximum steering, both inner and outer wheels, and no steering

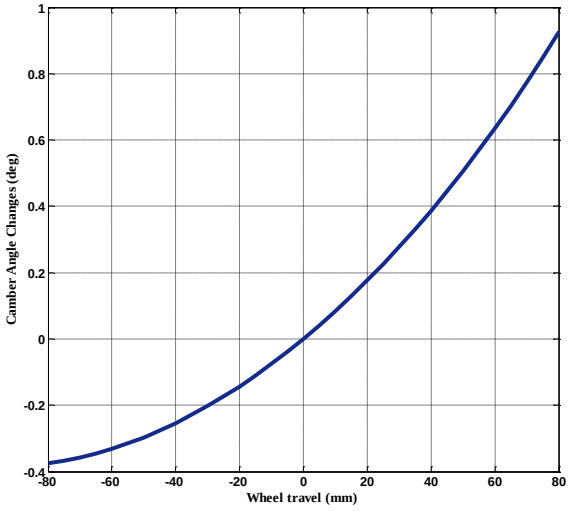

Figure 51- Camber angle changes by wheel travel

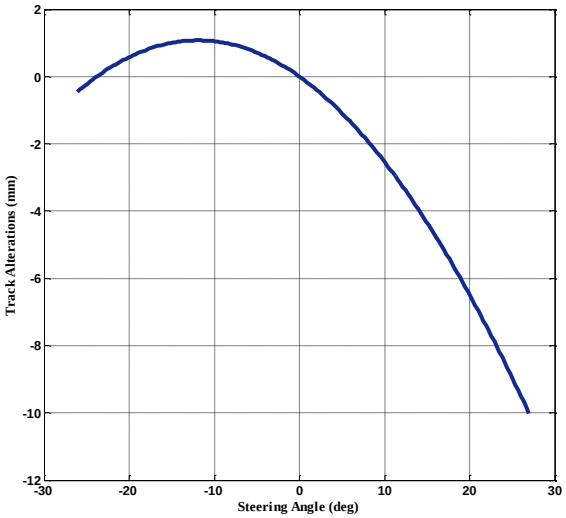

Figure 52-Track Alterations by steering

The last figure indicates the steering geometries of the initial guess and the optimized result along with the Ackermann and the parallel steering principles. As indicated, the final design is in great accordance with linear steering.

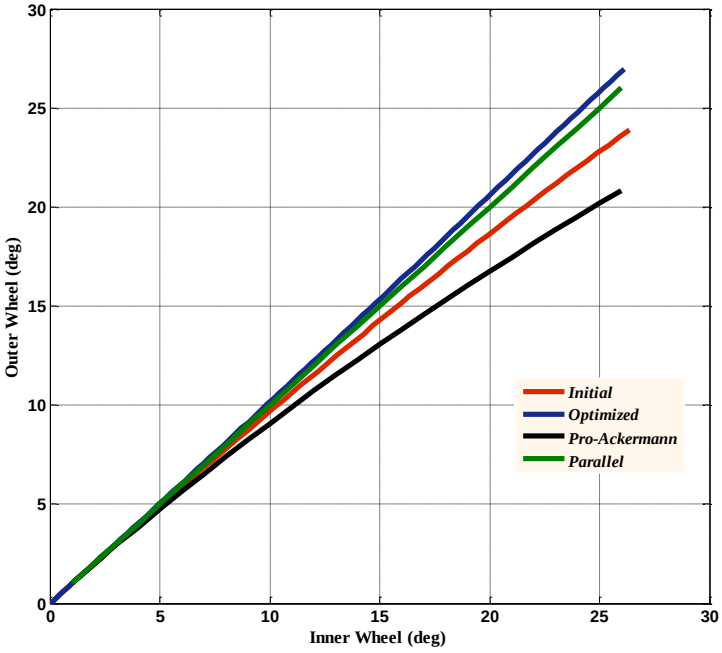

Figure 53- Steering Characteristics vs. Principles

Conclusion

In conclusion, this thesis tried to propose an optimal design for two widely used suspensions in regards of road holding and stability responsibility of the suspension. Two important factors that are usually neglected falsely are also considered in this study: steering and the priority of desired characteristics, both of which were explained after a detailed literature review. This study also proposed a combined method for modelling the mechanisms to reduce the number of equations. The modelling was also verified by comparing results with ADAMS and MapleSim software.

At last, three major case studies where done. At first, a practical study was done on a family car to defend the proposed claims about suspension characteristics. Then, the optimization method was verified and used for providing better behavior due to the vehicle's functionality. All the case studies showed great results and were in perfect accordance with expected road holding behavior of suspension which was studied and reviewed formerly.

Concerning the modelling done in this thesis, the proposed method can be used in further studies to solve the system faster and even linearize them for a 3D control study. Regarding the optimization, further studies can use this approach for different steering mechanisms or even add longitudinal dynamics to study a full car. Indeed, the fewer number of equations can result in less time consumption for solving a full car model. Also, studying the anti-roll bar effects can be easily added to analysis and optimization, along with optimizing the spring motion ratio.

Another interesting area of research for further studies would be in optimizing different types of multi-link suspensions with the same approach. Then, a comparison between different suspensions can create a more comprehensive body of knowledge of suspension technologies.

Altogether, both the modelling and the optimization used in this thesis met the desired expectations and can be used in many different areas of vehicle dynamics as well.

Bibliography

[1] Jazar RN. Vehicle Dynamics: Theory and Application. Springer; 2008.

[2] Dixon JC. Tires, suspension, and handling. Society of Automotive Engineers; 1996.

[3] Suspension Basics 1 - Why We Need It. Initial Dave n.d. http://www.initialdave.com/cars/tech/suspensionbasics01.htm (accessed June 26, 2015).

[4] Suspension Basics 3 - Leaf Springs. Initial Dave n.d. http://www.initialdave.com/cars/tech/suspensionbasics03.htm (accessed June 26, 2015).

[5] Double wishbone suspension n.d.:https://en.wikipedia.org/wiki/Double_wishbone_susp.

[6] Reimpell J, Stoll H, Betzler JW. The Automotive Chassis. Elsevier; 2001. doi:10.1016/B978-075065054-0/50013-4.

[7] Koch GPA. Adaptive Control of Mechatronic Vehicle Suspension Systems. Technical University of Munich, 2011.

[8] Eskandary PK. Interconnected Air Suspensions with Independent Height and Stiffness Tuning. University of Waterloo, 2014.

[9] Baumal AE, Mcphee JJ, Calamai PH. Application of genetic algorithms to the design optimization active vehicle suspension system. Comput Methods Appl Mech Eng 1998;163.

[10] Barak P. Magic Numbers in Design of Suspensions for Passenger Cars. 1991. doi:10.4271/911921.

[11] Stensson a., Asplund C, Karlsson L. The Nonlinear Behaviour of a MacPherson Strut Wheel Suspension. Veh Syst Dyn 1994;23:85–106. doi:10.1080/00423119408969051.

[12] Hurel J, Mandow A, Garc A. Nonlinear Two-Dimensional Modeling of a McPherson Suspension for Kinematics and Dynamics Simulation. 12th IEEE Int Work Adv Motion Control 2012.

[13] Fallah MS, Bhat R, Xie WF. New model and simulation of Macpherson suspension system for ride control applications. Veh Syst Dyn Int J Veh Mech Mobil 2009;47:195–220. doi:10.1080/00423110801956232.

[14] Andersen ER, Sandu C, Kasarda M. Multibody Dynamics Modeling and System Identification for a Quarter-Car Test Rig with McPherson Strut Suspension Multibody Dynamics Modeling and System Identification for a Quarter-Car Test Rig with McPherson Strut Suspension. Virginia Polytechnic Institute and State University, 2007.

[15] Raghavan M. Analysis Of Independent Suspension Linkages. Warren, Michigan: n.d.

[16] Simionescu PA, Beale D. Synthesis and analysis of the five-link rear suspension system used in automobiles. Mech Mach Theory 2002;37:815–32.

[17] Fallah MS, Mahzoon M, Eghtesad M. KINEMATICAL AND DYNAMICAL ANALYSIS OF MACPHERSON SUSPENSION USING DISPLACEMENT MATRIX METHOD. Iran J Sci Technol 2008;32:325–39.

[18] Lee HG, Won CJ, Kim JW. Design Sensitivity Analysis and Optimization of McPherson Suspension Systems. Proc World Congr Eng 2009;II.

[19] Attia HA. Dynamic modelling of the double wishbone motor-vehicle suspension system. Eur J ofMechanics A/Solids 2002;21:167–74.

[20] Liu X, Luo J, Wang Y, Guo H, Wang X. Analysis for Suspension Hardpoint of Formula SAE Car Based on Correlation Theory. Res J Appl Sci 2013;6:4569–74.

[21] Mántaras D a., Luque P, Vera C. Development and validation of a three-dimensional kinematic model for the McPherson steering and suspension mechanisms. Mech Mach Theory 2004;39:603–19. doi:10.1016/j.mechmachtheory.2003.12.006.

[22] Knapczyk J, Maniowski M. Elastokinematic modeling and study of five-rod suspension with subframe. Mech Mach Theory 2006;41:1031–47. doi:10.1016/j.mechmachtheory.2005.11.003.

[23] Knapczyk J, Maniowski M. Optimization of 5-rod car suspension for elastokinematic and dynamic characteristics. Arch Mech Eng 2010;LVII.

[24] Bael S, Lee JM, Chu CC. Axiomatic Design of Automotive Suspension Systems Sangwoo n.d.;0:1–4.

[25] Hwang JS, Kim SR, Han SY. Kinematic design of a double wishbone type front suspension mechanism using multi-objective optimization 1 Introduction 2 Kinematic analysis of a suspension mechanism. 5th Australas Congr Appl Mech 2007.

[26] Haug EJ. Intermediate dynamics. Prentice Hall PTR; 1992.

[27] Haug EJ. Computer Aided Kinematics and Dynamics of Mechanical Systems, Volume 1. Allyn & Bacon, Incorporated; 1989.

[28] Nikravesh PE. Computer-aided analysis of mechanical systems. Prentice-Hall; 1988.

[29] Sancibrian R, Garcia P, Viadero F, Fernandez A, De-Juan A. Kinematic design of double-wishbone suspension systems using a multiobjective optimisation approach. Veh Syst Dyn Int J Veh Mech Mobil 2010;48:793–813. doi:10.1080/00423110903156574.

[30] Thompson D. Ackerman ? Anti-Ackerman ? Or Parallel Steering ? n.d.

[31] Costin M, Phipps D. Racing and Sports Car Chassis Design. B. T. Batsford Limited; 1974.

[32] Smith C. Tune to Win. Carroll Smith Consulting; 1978.

[33] Smith C. Engineer in Your Pocket: A Practical Guide to Tuning the Race Car Chassis and Suspension. Carroll Smith Consulting; 1998.

[34] Staniforth A. Competition Car Suspension: A Practical Handbook, Fourth Edition. Haynes Publishing UK; 2006.

[35] Alexander D. Performance Handling. Motorbooks International; 1991.

[36] Valkenburg P Van. Race Car Engineering and Mechanics. Penguin Group (USA) Incorporated; 1992.

[37] Zapletal E. Ackerman. Race Car Eng 2001.

[38] Ruelle C. Race Car Engineering & Data Acquisition Seminar n.d.

[39] Ortiz M. THE MARK ORTIZ AUTOMOTIVE CHASSIS NEWSLETTER n.d.

[40] Ion P, Gheorghe C, Nicolae I. OPTIMIZATION STUDY OF A CAR SUSPENSION – STEERING LINKAGE n.d.

[41] Park S-J, Sohn J-H. Effects of camber angle control of front suspension on vehicle dynamic behaviors. J Mech Sci Technol 2012;26:307–13. doi:10.1007/s12206-011-1206-1.

[42] Felzein ML, Cronin DL. STEERING ERROR OPTIMIZATION OF THE MACPHERSON. Mech Mach Theory 1985;20:17–26.

[43] Habibi H, Shirazi KH, Shishesaz M. Roll steer minimization of McPherson-strut suspension system using genetic algorithm method. Mech Mach Theory 2008;43:57–67. doi:10.1016/j.mechmachtheory.2007.01.004.

[44] PEUGEOT TECHNOLOGY: Double Wishbone : Derivation and History n.d. http://groupsevenpeugeot.blogspot.ca/2012/10/double-wishbone-derivation-and-history.html (accessed June 26, 2015).

[45] Ludvigsen K. The Truth About Chevy's Cashiered Cadet. Spec Interes Autos 1974:16 – 19.

[46] Shoenberger RW. Human response to whole-body vibration. Percept Mot Skills 1972;34:127–60. doi:10.2466/pms.1972.34.1.127.

[47] Varterasian JH, Thompson RR. The Dynamic Characteristics of Automobile Seats with Human Occupants. 1977. doi:10.4271/770249.

[48] Van Deusen BD. Human Response to Vehicle Vibration. 1968. doi:10.4271/680090.

[49] Doumiati M, Victorino A, Charara A, Lechner D. A method to estimate the lateral tire force and the sideslip angle of a vehicle: Experimental validation. Proc. 2010 Am. Control Conf., IEEE; 2010, p. 6936–42. doi:10.1109/ACC.2010.5531319.

[50] Minh V. Vehicle Sideslip Modeling and Estimation. n.d.

[51] Automobile Ride, Handling, and Suspension Design n.d. http://www.rqriley.com/suspensn.htm (accessed June 28, 2015).

[52] Inside the Mercedes-Benz SLS AMG E-Cell supercar n.d. http://www.gizmag.com/mercedes-sls-amg-e-cell/21778/ (accessed June 29, 2015).

[53] Edgar J. Front Suspension Designs n.d. http://www.autospeed.com/cms/article.html?&A=2934 (accessed June 29, 2015).

[54] Longhurst CJ. Car Bibles : The Suspension Bible n.d. http://www.carbibles.com/suspension_bible.html (accessed June 29, 2015).

[55] Anti-Roll Bar | How It Works n.d. http://www.uniquecarsandparts.com.au/how_it_works_anti_roll_bar.htm (accessed June 29, 2015).

[56] Crolla DA. AUTOMOTIVE ENGINEERING: Powertrain, Chassis System and Vehicle Body. First. Elsevier; 2009.

[57] King-Hele D. Erasmus Darwin's Improved Design for Steering Carriages--And Cars on JSTOR. Notes Rec R Soc Lond 2002;56:41–62.

[58] Heißing B, Ersoy M. Chassis Handbook: Fundamentals, Driving Dynamics, Components, Mechatronics, Perspectives. vol. 9. Springer Science & Business Media; 2010.

[59] Rosth M. Hydraulic Power Steering System Design in Road Vehicles. Linkoping: 2007.

[60] Ogata K. Modern Control Engineering. Fifth. n.d.